ACS OMEGA

Open Access

This article is licensed under CC-BY-NC-ND 4.0

http://pubs.acs.org/journal/acsodf

Review

Metal/Covalent Organic Framework Encapsulated Lead-Free Halide Perovskite Hybrid Nanocatalysts: Multifunctional Applications, Design, Recent Trends, Challenges, and Prospects

Anam Altaf, Iltaf Khan,* Aftab Khan, Samreen Sadiq, Muhammad Humayun, Shoaib Khan, Saeed Zaman, Abbas Khan, Rasha A. Abumousa, and Mohamed Bououdina

Cite This: *ACS Omega* 2024, 9, 34220−34242

Read Online

ACCESS | Metrics & More | Article Recommendations

ABSTRACT: Perovskites are bringing revolutionization in a various fields due to their exceptional properties and crystalline structure. Most specifically, halide perovskites (HPs), lead-free halide perovskites (LFHPs), and halide perovskite quantum dots (HPs QDs) are becoming hotspots due to their unique optoelectronic properties, low cost, and simple processing. HPs QDs, in particular, have excellent photovoltaic and optoelectronic applications because of their tunable emission, high photoluminescence quantum yield (PLQY), effective charge separation, and low cost. However, practical applications of the HPs QDs family have some limitations such as degradation, instability, and deep trap states within the bandgap, structural inflexibility, scalability, inconsistent reproducibility, and environmental concerns, which can be covered by encapsulating HPs QDs into porous materials like metal−organic frameworks (MOFs) or covalent−organic frameworks (COFs) that offer protection, prevention of aggregation, tunable optical properties, flexibility in structure, enhanced biocompatibility, improved stability under harsh conditions, consistency in production quality, and efficient charge separation. These advantages of MOFs-COFs help HPs QDs harness their full potential for various applications. This review mainly consists of three parts. The first portion discusses the perovskites, halide perovskites, lead-free perovskites, and halide perovskite quantum dots. In the second portion, we explore MOFs and COFs. In the third portion, particular emphasis is given to a thorough evaluation of the development of HPs QDs@MOFs-COFs based materials for comprehensive investigations for next-generation materials intended for diverse technological applications, such as CO_2 conversion, pollutant degradation, hydrogen generation, batteries, gas sensing, and solar cells. Finally, this review will open a new gateway for the synthesis of perovskite-based quantum dots.

1. INTRODUCTION

Perovskites have gained significant attention in recent years due to their unique properties and potential applications in various fields, particularly CO_2 conversion, pollutant degradation, hydrogen generation, batteries, gas sensing, and solar cells.[1−4] Perovskites have the general formula ABO_3, and if we replace O with X they become more efficient HPs that exhibit excellent optical and electronic properties, including high absorption coefficients, long carrier diffusion lengths, and low defect densities.[5] However, among them, lead-based HPs have high toxicity and environmental concerns that need to be addressed, and researchers have developed LFHPs with the same properties as their lead-based counterparts.[6] However, HPs QDs have limited structural adjustability and poor stability against heat, oxygen, water, etc., limiting their use in various practical applications.[7] To overcome these shortcomings, many semiconductor materials have attracted considerable attention, including metal−organic frameworks (MOFs) and covalent−organic frameworks (COFs). MOFs are porous materials composed of metal ions or clusters coordinated to organic ligands, while COFs are crystalline porous polymers with extended π-conjugated frameworks.[8,9] They possess high surface areas, enhanced stability, and tunable pore sizes, making them suitable for coupling with HPs QDs to develop hybrid materials known as HPs QDs@MOFs-COFs.[10] By incorporating MOFs or COFs into HPs QDs, researchers have achieved enhanced performance in various practical applications such as CO_2 conversion, pollutant degradation, hydrogen generation, batteries, etc. In CO_2 conversion, HPs QDs@MOFs-COFs have shown great potential as catalysts, enabling the conversion of CO_2 into valuable chemicals or fuels by enhancing the catalytic activity

Received: May 13, 2024
Revised: July 16, 2024
Accepted: July 23, 2024
Published: August 1, 2024

© 2024 The Authors. Published by American Chemical Society

Table 1. Examples of Perovskites and Their Applications

Perovskite type	Synthesis method	Nature	Applications	Output	Ref.
$GdFeO_3$	Solution Based	Perovskite nanorods	Pollutant degradation and CO_2 conversion	High surface area and enhanced catalytic activity	23
$CaTiO_3$	Hydrothermal	Perovskite	Thermoelectric ceramics	Lowcost and eco-friendly	17
$CoMoO_4$/CoMoB	Solvothermal	Boron doped perovskite	Electrocatalytic water splitting	Enhanced electroconductivity	18
SrO/$LaFeO_3$	One-pot	SrO/Perovskite	Organic pollutant degradation and CO_2 conversion	High charge separation and surface activity	20
$CH_3NH_3PbI_{3-x}Cl_x$	Spin coating	Perovskite	PSCs	Better crystallinity and large size	38
$La_{0.4}Sr_{0.6}Co_{0.7}Fe_{0.2}Nb_{0.1}O_{3-\delta}$	Sol–gel	Perovskite	Energy storage	High stability and power density	39
$CH_3NH_3PbX_3$	Ligand-assisted	HP nanocrystals	Photodetectors	Self-powered and DMF, good solvent for synthesis	26
La–Sr–Co	Mechanochemical	Perovskite composite	Degradation	High catalytic degradation and nontoxic	28
$PbCl_2$/PbICl	CVD	Mixed HPs	PSCs	Grains size >2 μm	29
$PrBaMn_{0.5}Fe_{1.5}O_{5+\delta}$/FDC	ALD	CeO_2 decorated perovskite	Fuel cells	Improved electrocatalytic activity	30
SnO_2/$LaFeO_3$	Template–adsorption–calcination	Yolk shell perovskite coupled with SnO_2	Photocatalytic degradation	High charge separation	33
MA_2SnCl_6	-	HPs	Energy storage and harvesting	High capacity and stability	37

and stability, leading to improved CO_2 conversion efficiency. In this regard, Wang et al. reported $CsPbBr_3$@PCN-222 as a photocatalyst for CO_2 reduction which demonstrated 2.1 times improvement in CO_2 to HCOOH.[11] Pollutant degradation is another application where HPs QDs@MOFs-COFs have demonstrated significant potential as they can effectively degrade pollutants in water or air through photocatalytic or adsorption processes due to their large surface area and efficient charge transfer pathways.[12] Very recently, Ai and co-workers utilized $CsSnBr_3$@ZIF-67 for effective malachite green pollutant degradation.[13] Moreover, hydrogen generation is a key process for clean energy production, in which HPs QDs@MOFs-COFs have been explored as photocatalysts for water splitting due to enhanced light absorption and charge separation, leading to improved hydrogen generation efficiency. In addition, Meng et al. reported a variety of HPs QDs ($CsPbBr_3$, $CsPbBr_2I$, ESY-$CsPbBr_3$, and RB-$CsPbBr_2I$)@COF-SH for photocatalytic activities (such as degradation, hydrogen generation, etc.) and have light-harvesting capability for higher yields.[14] HPs QDs@MOFs-COFs also have significant potential in the field of batteries, solar cells, and sensors.[15,16] Based on the above discussion, it is a hot and emerging research field. Further research and development in this area are expected to unlock the full potential of HPs QDs@MOFs-COFs and pave the way for advanced technologies with enhanced performance and sustainability.

2. EXPLORING PEROVSKITES

Perovskites make up a class of materials with a unique crystal structure that gives rise to their exceptional properties. The perovskite name was given after the mineral, whose chemical formula is $CaTiO_3$.[17] ABO_3 is the general formula of perovskites, where A and B signify different metal cations and O corresponds to an anion, typically oxygen.[18,19] The A-site cation consists of different elements, like earth metals (e.g., calcium, strontium) or alkaline rare earth metals (e.g., lanthanum, neodymium).[20] Transition metal ions are generally utilized as B-site cations.[21,22] The perovskite structure is characterized by a three-dimensional arrangement of metal cations surrounded by an octahedral cage of oxygen anions.[23] Notably, perovskites have the ability to undergo structural phase transitions that occur in response to external conditions like temperature and pressure. For example, the perovskite phase transition from a cubic phase to an orthorhombic or tetragonal phase is the most studied transition which often comes from the changes in physical parameters, e.g., magnetic ordering and electrical conductivity, etc.[24] The flexibility in the perovskite structure allows a variety of elements to be incorporated into its lattice, resulting in the innovation of a wide range of perovskites with distinct properties; e.g., perovskite oxides are utilized in fuel cells and catalytic converters due to their efficient catalytic activity. There are many approaches used for the synthesis of perovskites, as shown in Table 1 and Figure 1. Mostly solution-based methods

Figure 1. Overview of the applications, morphology, properties, and synthesis of perovskites.

are used for the preparation of perovskite materials due to their versatility and simplicity. The sol–gel technique is the most utilized solution-based method. In this approach, a precursor solution consisting of metal–organic compounds or metal salts is mixed with a solvent to prepare a sol. The sol is then subjected to a gelation process, which can be achieved through

https://doi.org/10.1021/acsomega.4c04532
ACS Omega 2024, 9, 34220–34242

Table 2. Examples of HPs and Their Applications

Halide perovskite type	Synthesis method	Nature	Applications	Output	Ref.
$Cs_3Cu_2X_5$	Hot injection method	Metal HPs	Light emission compounds	PL quantum yield exceeding 90%	48
$(BA)_2(MA)_{n-1}Pb_nI_{3n+1}$	Spin-coating and scalable blading	3D-like perovskites	High-performance devices (solar cells)	Enhanced PCE	51
$Cs_2AgBiBr_6$	Microwave-assisted solvothermal	Double perovskite nanoparticles	Optoelectronic	Promising moisture and thermal stability	52
α-$FAPbI_3$	Vapor deposition	Lead-based HP	Solar cell	PCE over 20%	53
α-$FAPbI_3$	Solution based	HP	Semiconductor	More efficient carrier transport	54
Cs_2AgBiI_6	Simple antisolvent approach	LFHP	Pollutant degradation	High photocatalytic performance	56
g-C_3N_4/$CsPbBr_3$	Hot injection method	HP nanocrystals	CO_2 photoreduction and water splitting	Enhanced charge separation	57
$CH_3NH_3PbBr_3$@TiO_2	Solution based	HP QDs	Photoelectrochemical sensor	Water stability	60

various techniques, such as hydrolysis or condensation reactions. The gel obtained is dried and then calcined at high temperatures to get the required perovskite material.[25] One more solution-based technique is the precipitation method, which requires the controlled precipitation of metal ions from a solution consisting of suitable precursors. Usually, two separate solutions containing the A-site and B-site precursors are prepared and mixed under controlled conditions. The reaction between the precursors allows the formation of insoluble perovskite nanoparticles that can be collected by centrifugation or filtration and further processed to obtain the final product.[26] The second one is solid-state techniques, which involve the direct reaction between solid precursors to prepare perovskite materials. The most employed solid-state techniques are the ceramic or solid-state reaction method. In this method, the starting materials, normally carbonates or metal oxides, are completely mixed and heated at high temperatures to promote the diffusion of ions and the formation of the perovskite phase. The temperature profile and reaction kinetics play a vital role in determining the crystallinity and phase purity of the final product.[27] Another type of solid-state method is ball milling or mechanochemical synthesis, in which precursors are added to the ball mill, and then mechanical forces are applied by milling balls. Due to these high-energy collisions between precursors and balls, perovskite is formed. Mechanochemical synthesis has various advantages such as lower reaction temperature, shorter reaction times, and final product homogeneity.[28] Now we discuss the vacuum-based methods in which precursor vapors are deposited on a substrate by annealing to prepare perovskite films. The most commonly used vapor-based methods are chemical vapor deposition (CVD) and atomic layer deposition (ALD). In CVD, suitable carrier gas and precursors are added in the reaction chamber at high temperatures, which leads to the perovskite film deposition on the heated substrate. CVD gives good control over composition and film thickness which makes it suitable for commercial scale.[29] ALD involves substrate exposure to different precursors in the form of vapors which lead to the controlled growth with atomic precision of films.[30] Overall, perovskite synthesis needs careful control over several parameters including solvent selection, precursor choice, annealing conditions, and the film deposition method, which significantly affect the structure, properties, and final composition of perovskites. Due to their unique properties, perovskites have been uncovered in various fields, e.g., solar cells and catalysis, where they have shown great capability as efficient photovoltaic and low-cost materials. Additionally, Tan and his team prepared the $CsPbI_3$ solar cell which has enhanced stability, temperature reliability, and improved photovoltaic properties.[31] Moreover, perovskite solar cells (PSCs) have achieved high power conversion efficiencies (PCEs) comparable to traditional silicon-based solar cells.[32] Furthermore, perovskite catalysts are used in various reactions including oxygen reduction reactions in pollutant degradation, water splitting, fuel cells for hydrogen production, and CO_2 conversion for renewable energy storage. In addition, Khan et al. synthesized $LaFeO_3$-based nanocomposite as an efficient photocatalyst for 2,4-dichlorophenol dye degradation.[33] Perovskites also find great potential in gas sensing due to their high sensitivity and surface area which enables perovskites to detect various gases like carbon monoxide (CO), nitrogen dioxide (NO_2), and volatile organic compounds (VOCs) at low concentrations, making them suitable for industrial safety, healthcare, and environmental monitoring applications.[34,35] Also, perovskites have also shown potential in magnetic storage devices such as high-temperature superconductors, solid-state batteries, and solid oxide fuel cells due to their efficient ion conduction, magnetism, superconductivity, and thermoelectricity.[36] Very recently, Li et al. used a perovskite ($CsPbI_2Br$) photovoltaic module to prepare solid-state Li−S batteries which exhibited high storage and conversion efficiency.[37] Regardless of their potential, there are still some limitations such as scalability and stability that need to be addressed. Perovskites are sensitive to oxygen and moisture, which reduces their performance over time. Researchers are keenly working on developing approaches to improve the stability of perovskite materials and make them more suitable for large-scale applications.

3. INVESTIGATING HALIDE PEROVSKITES

HPs have been getting a significant spotlight in recent years due to their exploited optoelectronic properties and potential applications such as solar cells, lasers, CO_2 conversion, pollutant degradation, water splitting, field effect transistors, etc.[40,41] HPs are donated by the general formula ABX_3, where the A cation is typically an organic or inorganic cation, while the B cation is a metal−cation and X a halide anion. Halides provide more degrees of freedom to the perovskite structure, which may be used to adjust the material's characteristics.[42] HPs are more adaptable for a range of applications since the presence of halides may alter the material's bandgap, carrier mobility, and stability. In the HPs structure, the A cations occupy the corners of a cube, while the X anions occupy the face centers of the cube. The B cations are located at the center of the cube.[43] This arrangement creates a three-dimensional network of corner-sharing BX_6 octahedra, where each B cation

https://doi.org/10.1021/acsomega.4c04532
ACS Omega 2024, 9, 34220−34242

is surrounded by six X anions. The octahedra formed by the BX_6 units give rise to several important structural features of the HPs. First, these octahedra can tilt or rotate relative to each other, leading to different structural distortions.[44] In various cases, this tilting shows outcomes such as lower symmetry structures like tetragonal ($CsSrCl_3$), monoclinic ($Rb_3Sb_2I_9$), and orthorhombic (Cs_3BiI_6).[45] For example, orthorhombic $CsPbI_3$ shows higher octahedral tilting as compared to tetragonal $CsPbI_3$.[46] These distortions can impact the optical and electronic properties of the material. Moreover, interstitial spaces or voids are created by corner-sharing of octahedra within the crystal structure which can accommodate additional molecules that can improve HPs properties such as device performance and stability.[47] The interstitial spaces created by the BX framework are occupied by A-site cations, which serve as a pillar to the perovskite structure stability. Also, HPs can show various types of bonding interactions including partially covalent and purely ionic depending on the combination of elements at A, B, and X sites. The bond nature affects the charge transport and electronic band properties of HPs.[48] For example, different band gaps can be accomplished by changing the A-site cation, which helps in tuning the emission and optical absorption properties. Moving on the synthesis of HPs involves the preparation of high-quality crystalline nanorods, QDs, nanoparticles, or films with controlled morphology and composition.[49] There are various synthesis methods used for HPs preparation, such as high-temperature, hybrid, and wet chemical approaches, as shown in Table 2 and Figure 2. Wet

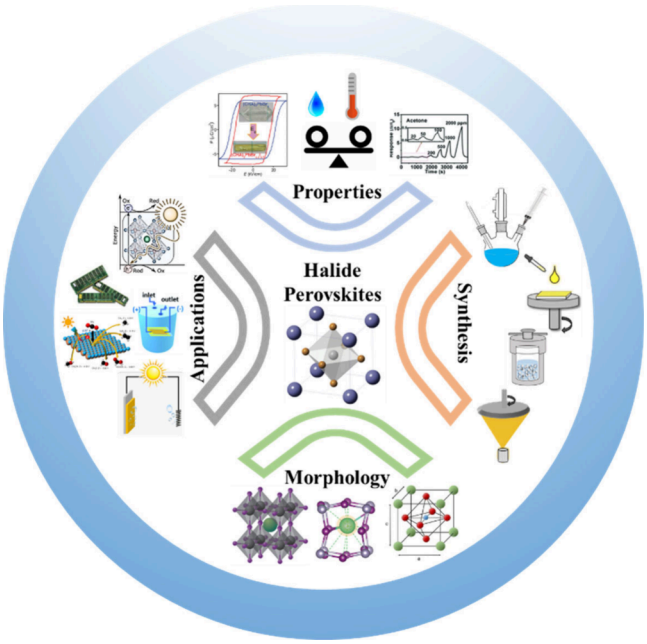

Figure 2. Overview of the applications, morphology, properties, and synthesis of HPs.

chemical methods include solution-based, solvothermal, and hydrothermal approaches. The solution-based technique is the most commonly used wet chemical method which further includes inkjet printing, spin coating, and doctor blading techniques.[50] In this approach, the precursor is deposited on a substrate, and then the solvent is removed by heating. The final film formed can be further annealed at low temperatures to improve the optoelectronic properties and crystallinity.[51] The second wet chemical method is solvothermal which involves the metal halide reaction with organic ligands at temperature and pressure that control the morphology and crystal growth of perovskites.[52] The third technique is the hydrothermal technique in which the precursor solution is heated in an autoclave under high pressure. Moving forward, high-temperature processes consist of solid-state reactions and vapor-assisted deposition that typically involve the reaction of solid-state precursors at high temperatures to prepare the desired perovskite phase.[53] In addition to high-temperature and wet chemical methods, there are techniques for HPs synthesis, e.g., electrospinning and CVD. As we know, the HPs structure is highly versatile and can accommodate a wide range of compositions and substitutions. This flexibility allows for the engineering of HPs with desired properties for various applications.[54] One of the notable applications of HPs is in the removal of pollutants. These materials have shown promising results in the photocatalytic degradation of organic pollutants, such as dyes and pesticides, through the generation of reactive oxygen species (ROS) under light irradiation.[55] Very recently, Huang et al. prepared Cs_2AgBiI_6-GO with high stability for effective organic pollutant photocatalytic degradation.[56] HPs have also been explored for photocatalysis, where they can efficiently convert solar energy into chemical energy for various reactions, including water splitting, to produce hydrogen fuel. In this regard, Laishram and his research team synthesized water- and air-stable g-C_3N_4/$CsPbBr_3$ for water splitting and CO_2 photoreduction.[57] This application holds great potential for renewable energy production. Furthermore, HPs have demonstrated excellent performance in ions and gas sensing.[58] Their high surface-to-volume ratio and tunable bandgap make them suitable for detecting a wide range of ions and gases with high sensitivity and selectivity.[59] This capability opens up new possibilities for environmental monitoring, industrial safety, and healthcare applications. A team of researchers prepared a novel $CH_3NH_3PbBr_3$@TiO_2 photoelectrochemical sensor for cholesterol detection with facile, high sensitivity, and low cost approach.[60] HPs with ferroelectric properties have also been studied for applications like memory devices, sensors, actuators, and energy storage systems.[61] Despite the tremendous progress made in the field of HPs, there are still ceratin challenges that must be addressed before their widespread commercialization. One major concern is the stability and deep trap states within the bandgap of these materials, as they tend to degrade when exposed to moisture or heat and hinder the charge carrier dynamics. Efforts are underway to develop encapsulation techniques and improve the stability of HPs. Another challenge is the toxicity of lead-based perovskites, which has raised environmental concerns. Researchers are actively exploring alternative compositions that are lead-free while maintaining similar properties.

In summary, perovskites of the common variety (ABO_3) have numerous advantages compared to their halide counterparts (ABX_3). These materials exhibit excellent thermal and chemical stability, making them highly suitable for long-term use in a wide range of environmental conditions. In addition, ABO_3 materials are frequently found in larger quantities and are more affordable, leading to reduced production expenses. They are more environmentally friendly because they do not contain toxic halide components, which can be difficult to dispose of and recycle. Moreover, perovskites of the ABO_3 variety exhibit superior mechanical properties, such as

https://doi.org/10.1021/acsomega.4c04532
ACS Omega 2024, 9, 34220−34242

Table 3. Examples of LFHPs and Their Applications

LFHPs type	Synthesis method	Nature	Applications	Output	Ref.
Cs_2TeBr_6	Hydrothermal	Inorganic LFHP	c sensors	Good repeatability, stability, and short response time (4 s)	62
$(PEA)_4AgBiBr_8$, $(PEA)_2CsAgBiBr_7$, $Cs_2AgBiBr_6$	Slow crystallization	Double LFHP	Light emitting	Weak dimensional confinement	63
$Cs_3Bi_{2x}Sb_{2-2x}I_9$	-	LHHP	Hydrogen evolution	High optical absorption and stability	64
$Cs_3Sb_2Cl_3Br_6$	Solution based	LHHP	Self-powered photodetector	High responsivity (1 $\mu A \cdot W^{-1}$)	66
$MA_3Bi_2I_9$, $MA_3Bi_2I_6Br_3$, $MA_3Bi_2I_6Cl_3$	CVD	LFHP	Photodetector	Flexible, self-powered, and stable	68
Cs_2TeCl_6	Mechanochemical	LFHP	Stress recording	Reported the first time and has irreversible recording and long storage time	69
$Cs_3Sb_2Br_9$	Antisolvent	LFHP hollow nanospheres	CO_2 reduction	Efficient photocatalytic activity	71
$Cs_2AgInCl_6$	Precipitation	Double LFHP	Organic pollutant degradation	Highly stable and efficient	73
$CsSn_{1-x}Ge_xI_3$		LFHP	Solar cells	Twice PCE	74
$(iBA)_2(MA)_3Pb_4I_{13}$	Spin-coating	Hybrid LFHP	Rechargeable batteries	91% retention	79

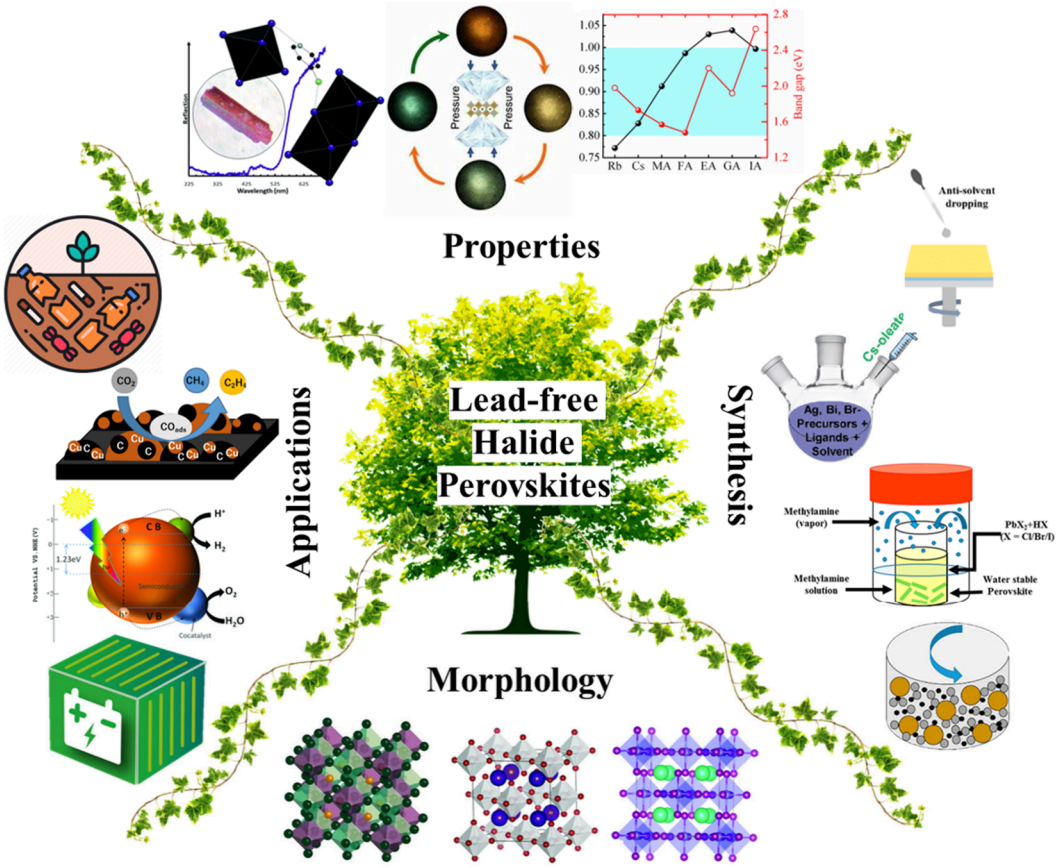

Figure 3. Overview of the applications, morphology, properties, and synthesis of LFHPs.

increased hardness and resilience, which render them highly suitable for structural applications. They have a wide range of applications beyond photovoltaics.

4. UNDERSTANDING LEAD-FREE HALIDE PEROVSKITES

Lead-based HPs have gained significant attention in the field of optoelectronics due to their exceptional photovoltaic properties. However, the presence of lead in these materials raises concerns regarding their environmental impact and potential health hazards. For this reason, lead-free halide perovskites (LFHPs) are hotspots in the research field. Additionally, the structure of LFHPs is similar to that of their lead-based counterparts.[62] They consist of a 3D crystal lattice with an organic cation, inorganic metal halides, and an additional component to stabilize the structure. The absence of lead necessitates the incorporation of alternative elements such as tin (Sn), germanium (Ge), bismuth (Bi), or antimony (Sb) into the crystal lattice.[63] Chen and his co-workers prepared LFHP ($Cs_3Bi_{2x}Sb_{2-2x}I_9$) for photocatalytic hydrogen evolution (PHE) and compared it with lead-based HP ($(CH_3NH_3)PbI_3$) which demonstrated that $Cs_3Bi_{2x}Sb_{2-2x}I_9$ has better efficiency

https://doi.org/10.1021/acsomega.4c04532
ACS Omega 2024, 9, 34220−34242

Table 4. Examples of HPs QDs and Their Applications

HPs QDs type	Synthesis method	Nature	Applications	Output	Ref.
$APbX_3$	Hot injection	HPs QDs	LEDs	High PLQY and binding energy	85
$CsPbX_3$	Hot injection	HPs QDs	Laser, LEDs, and solar cells	Improved stability in the external environment	105
$CsPb_{1-x}Sn_xBr_3$	Room temperature	HPs QDs	LEDs	High PLQY and stability	87
$CsPbBr_3$ QDs/PMMA	Ball milling	HPs QDs	LEDs and solar cells	High PLQY and stability	89
$CsPbX_3$	Microwave based	HPs QDs	Sensors	Tunable photoluminescent emissions	90
Zr-doped $CsPbBr_3$-KSCN	In-situ and solution based	HPs QDs	Green LEDs	Low toxicity, external quantum efficiency of 13.8%, and brightness of 24800 cd m^{-2}.	92
α-$CsPbI_3$	Facile	HPs QDs	Solar cells	8.28% PCE	94
$CsPbI_xBr_{3-x}$	Room-temperature recrystallization	3D HPs QDs	CO_2 reduction	Improved photocatalytic reaction	97
$MnSnO_2$@$CsPbBr_3$	Solvothermal	HPs QDs	Pollutant degradation	85.74% degradation rate	99
Cs−Cu−Cl	Sonochemical and in situ	HPs QDs	H_2 evolution	High stability	101
NS-$CsPbBr_3$	One pot	HPs QDs	Biomedical	Outstanding results in gas, chemo-, and photothermal therapies	102

for hydrogen production due to enhanced optical absorption than $(CH_3NH_3)PbI_3$.[64] Also, several factors that influence the morphology and structure of LFHPs such as the choice of cation and anion composition, precursor stoichiometry, solvent choice, processing conditions, additives or dopants, and substrate choice all play crucial roles in determining the morphology, crystallinity, and stability of these materials. Understanding and optimizing these factors are essential for developing high-performance LFHP-based materials.[65] For the synthesis of LFHP single crystals, colloids, and thin films, various methods such as solution-based, vapor-based, and solid-state methods can be employed, as shown in Table 3 and Figure 3. Solution-based methods are commonly used for synthesizing LFHP single crystals and colloids. One of the most commonly used solution-based methods is the hot injection technique. In this method, a precursor solution containing the organic cation, metal halide, and solvent is heated to a high temperature. Then, a second solution containing a reducing agent is rapidly injected into the precursor solution under vigorous stirring. The growth and nucleation of LFHP colloids or crystals can be prompted by rapid injection. Finally, colloids or crystals obtained can be purified and characterized for several applications. In this regard, Pramod et al. produced LFHP ($Cs_3Sb_2Cl_3Br_6$) by a solution-based method and utilized it for photodetectors.[66] One more solution-based approach is the antisolvent vapor-assisted crystallization technique in which the precursor solution is spin-coated on the substrate and then exposed to antisolvent vapor, e.g., toluene, chlorobenzene, etc. These vapors diffuse into the precursor film to form the LFHP film. This approach helps in controlling the crystallinity and morphology of film by varying antisolvent vapor exposure time and concentration.[67] There are vapor-based techniques as well such as CVD used to prepare LFHP films where volatile precursors react and deposit on the substrate in a reaction chamber. With this approach, film thickness, crystallinity, and composition can be optimized by controlling deposition parameters like pressure, precursor flow rate, and temperature.[68] The third one is the solid-state techniques, which are generally used for thin films and single crystals because of their compatibility, scalability, and simplicity, but they are less efficient than vapor-based and solution-based techniques. One of the most used solid-state techniques is grinding in which the precursor is ground and annealed at high temperatures.[69] Notably, the choice of synthesis approach depends on factors such as required morphology, specific application, and scalability. LFHPs are environmentally friendly and have demonstrated potential in different applications including pollutant degradation, energy storage, and CO_2 conversion.[70] In CO_2 conversion, LFHPs can be employed as catalysts to convert CO_2 into useful fuels or chemicals by photo-electrochemical reactions because their high surface area and exceptional electronic properties make them competent for capturing and utilizing solar energy. Very recently, Mu et al. synthesized hollow $Cs_3Sb_2Br_9$ which exhibited enhanced charge separation, surface activity, and photoresponse in photocatalytic CO_2 reduction.[71] Moreover, LFHPs have shown exceptional performance in pollutant degradation applications. They can be utilized as photocatalysts to break down organic pollutants in air or water by utilizing solar energy. This capability makes them promising candidates for addressing environmental pollution and improving the quality of air and water resources.[72] Also, a team of researchers synthesized a highly stable and efficient lead-free $Cs_2AgInCl_6$ photocatalyst for organic pollutant degradation.[73] Additionally, LFHPs have shown potential in battery technologies. Their ability to store and release charge efficiently makes them suitable electrodes materials in rechargeable batteries. By replacing the lead-based materials with lead-free alternatives, the safety and sustainability of battery systems can be enhanced. In addition, solar cells based on lead HPs have achieved remarkable PCEs exceeding 25%.[74] However, the toxicity and instability associated with lead-based HPs have motivated researchers to discover alternative materials. LFHPs, such as tin-based (e.g., methylammonium tin iodide) and bismuth-based (e.g., methylammonium bismuth iodide) perovskites, have shown promising photovoltaic properties.[75,76] These materials exhibit suitable bandgaps, high absorption coefficients, and long carrier lifetimes, making them attractive for solar cell applications.[77,78] Although the PCEs of LFHP solar cells are currently lower than their lead-based counterparts, ongoing research efforts aim to enhance their performance and stability.[79] Conversely, challenges related to stability, performance, scalability, and cost-effectiveness need to be overcome for their widespread adoption. Continued research and development efforts are crucial in unlocking the full potential of LFHPs for sustainable and eco-friendly technologies.

https://doi.org/10.1021/acsomega.4c04532
ACS Omega 2024, 9, 34220−34242

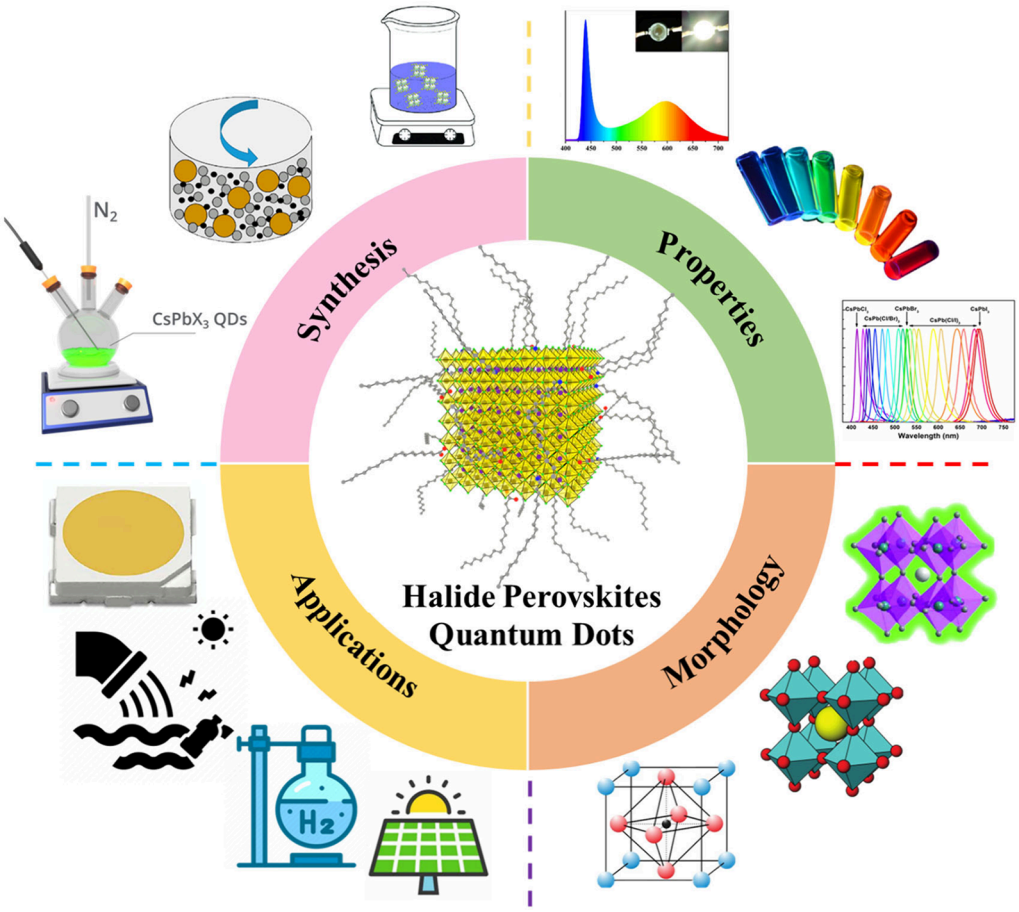

Figure 4. Overview of the applications, morphology, properties, and synthesis of HPs QDs.

5. COGNITION OF HALIDE PEROVSKITE QUANTUM DOTS

Artificial nanoscale crystals known as "quantum dots" have special optical and electrical characteristics, such as the capacity to move electrons and release a range of colored light when exposed to ultraviolet light.[80] HPs QDs are a class of nanoscale materials that have attained significant recognition in recent years due to their unique properties and potential applications in various fields, including optoelectronics, photovoltaics, and light-emitting devices.[81] Inorganic HPs QDs are a subclass of HPs QDs that consist solely of inorganic components which offer various benefits over organic−inorganic counterparts like high PLQY, tunable bandgap, improved charge transport, and enhanced stability.[82] Also, the inorganic nature of HPs QDs makes them more suitable for applications that need long-term stability, such as optoelectronic devices. HPs QDs have a similar crystalline structure to large-scale perovskite materials but at the nanoscale with reduced dimensions.[83] The HP QD general formula is ABX_3, where A shows an inorganic or organic cation; B shows a metal−cation; and X shows a halide anion.[84] HPs QDs which are most studied contain a combination of halides such as I, Cl, or Br as the anion and Sn or Pd as a metal−cation. HPs QDs form crystalline three-dimensional structures with the help of BX_6 octahedra. Inorganic or organic cations occupy the A site in the crystal lattice. Notably, we can precisely control the composition and size of QDs during their synthesis, allowing us to tune their optoelectronic properties.[85] Typically, HPs QDs demonstrate cubic or spherical morphology, with sizes ranging from a few to tens of nanometers. Furthermore, recent advances in synthesis techniques such as encapsulation and surface passivation strategies have enhanced the stability of HP QDs against heat, light, and moisture.[86] Moving forward, the synthesis methods of HPs QDs consist of room temperature and hot injection techniques as shown in Table 4 and Figure 4. The hot injection approach further consists of solvothermal and colloidal methods that offer precise control over morphology, composition, and size but involve high temperatures and utilize inert gases which make it unsuitable and cost-ineffective for the commercial scale.[87] While the room temperature approach consists of cation exchange reactions and ligand-assisted reprecipitation, it provides scalability and simplicity but has stability and size control limitations. As a result, the community of researchers is trying to explore various techniques that can help to prepare HPs QDs under ambient conditions.[88] Ball milling or grinding is one of these techniques that involves the mechanical grinding of solid precursors by using ligand or solvent. This approach provides various benefits such as offering QDs with narrow-size distributions, scalability, simplicity, synthesis at room temperature, no use of inert gases, and cost-effectiveness.[89] Another such technique is microwave irradiation, in which the precursor solution is subjected to microwave radiation. This approach encourages rapid heating, high yields, good particle size control, and fast reaction rates.[90] It also removes the requirement for inert gases and high temperatures, making it a good alternative to the hot injection method. HPs QD's unique properties (such as stability, optical, and electronic) make

https://doi.org/10.1021/acsomega.4c04532
ACS Omega 2024, 9, 34220−34242

Table 5. Examples of Common MOFs and Their Applications

MOF type	Synthesis method	Nature	Applications	Output	Ref.
UiO-66	Solvothermal	3D MOF	Pollutant removal	96% removal efficiency	108
Fe-MOF	Hydrothermal	MOF	Urea oxidation and water splitting	High stability and activity	111
Ce-La-MOFs	Hydrothermal	MOF	Adsorption	Removal efficiency is more than 90%	112
NiCo-MOF-74	Microwave-assisted	Bimetallic MOF	CO_2 capture	High uptake and selectivity for CO_2	113
$CsPbBr_3$/MOF-808	Mechanochemical	HP/MOF-808	Photocatalytic	Efficient removal under visible light	114
Zr-MOF	Sonochemistry	Nano popcorns	Tumor thermal therapy	120% higher temperature change value as compared to UIO-66	115
Fe(II) MOFs	Solution based	MOF	Degradation	Degradation rates up to 91.96%	117
Zr-MOF	Surfactant-assisted	Microspheres	Adsorption of uranium	1.75 times adsorption capacity than UiO-66-AO	120
3D-ZGC	-	MOF	Batteries	High stability, long-term cycling, and low cost	121

them attractive for various fields.[91] In optoelectronics, they have been utilized as active materials in LEDs, where their tunable emission properties enable the generation of different colors. Moreover, Yang et al. synthesized improved green LEDs by using Zr−Pb doped $CsPbBr_3$ QDs that showed enhanced operating half-life and external quantum efficiency.[92] They have also been incorporated into solar cells as light-absorbing materials due to their high absorption coefficients and long carrier diffusion lengths.[93] Very recently, Yang and his team prepared α-$CsPbI_3$ QDs for solar cell applications with a PCE of 8.28%.[94] In recent years, HPs QDs have gained significant attention as photocatalysts in the fields of CO_2 conversion, pollutant degradation, and hydrogen generation. HPs QDs have shown great potential in CO_2 conversion through photocatalytic reduction.[95] When exposed to light, these QDs can absorb photons and generate electron−hole pairs. The excited electrons can then participate in the reduction of CO_2 to produce valuable fuels or chemicals, such as CH_4, CH_3OH, or HCOOH.[96] The efficiency of CO_2 conversion using HPs QDs as photocatalysts has been demonstrated in several studies. Cheng et al. synthesized $CsPbI_xBr_{3-x}$ QDs for efficient photocatalytic CO_2 reduction which displayed enhanced reactions.[97] HPs QDs also exhibit excellent photocatalytic activity for the degradation of various pollutants present in air or water. These QDs can effectively generate ROS under light irradiation, which can oxidize and decompose organic pollutants into harmless byproducts. For example, HPs QDs have been used for the degradation of organic dyes, pharmaceutical compounds, and even persistent organic pollutants (POPs) such as polychlorinated biphenyls (PCBs). The high surface area and efficient charge separation properties of these QDs contribute to their enhanced photocatalytic performance.[98] A team of researchers utilized $CsPbBr_3/MnSnO_2$ QDs for the photocatalytic degradation of organic pollutants which demonstrated an 85.74% degradation rate.[99] HPs QDs have also shown promise as photocatalysts for hydrogen generation via water splitting. By absorbing photons, the QDs can generate electron−hole pairs, where the excited electrons can reduce protons (H^+) from water to produce H_2 gas.[100] The unique electronic structure and efficient charge transfer properties of HPs QDs enable them to achieve high hydrogen evolution rates. Notably, Li et al. synthesized photocatalyst Cs−Cu−Cl QDs with enhanced stability to use for H_2 evolution.[101] This shows their potential in future storage and energy conversion systems.[102] Moreover, HPs QDs have demonstrated potential in sensing and bioimaging fields due to their brilliant photoluminescence properties.[103] However, various limitations, such as instability and degradation under ambient conditions, need to be dealt with before their use as photocatalysts. The instability problem occurs due to the intrinsic HPs nature which can be improved by encapsulating them.[104] Moreover, the reproducibility and scalability of HPs QDs with consistent quality at the commercial scale remain vital problems. To overcome these challenges, the encapsulation of HPs QDs in or with COFs or MOFs can help address these problems and improve their performance.

6. METAL−ORGANIC FRAMEWORKS

In recent years, MOFs have been getting a lot of attention from the research community due to their distinctive properties and potential applications in several fields such as separation, gas storage, sensing, and catalysis.[106,107] The highly porous structure of MOFs consist of clusters or metal ion coordination with organic ligands. MOF dimensions can be modified by the shape and size of organic ligands and clusters of metal ions used. Generally, MOFs have a 3D structure with pores. The shape and size of these pores can be varied depending on ligands which allow for selective molecules or gas separation and adsorption.[108] MOFs can be classified into one-dimensional (1D), two-dimensional (2D), and three-dimensional (3D) depending on the connectivity between the ligands and clusters or metal ions.[109] In 1D MOFs, metal ion linear chains are connected with organic ligands. In the case of 2D MOFs, a network of ligands and metal ions is formed. MOFs consist of various types depending on the ligands or metal ions, e.g., pillared layered (PL), UiO type, zeolitic imidazolate frameworks (ZIFs), etc. PL is composed of metal−organic layers linked through organic pillars, while UiO consists of zirconium ions directed with ligands based on carboxylate.[110] ZIFs are made of zinc ions linked with ligands based on imidazole. Some commonly studied MOFs include HKUST-1 ($Cu_3(BTC)_2$), MIL-53 (Al), UiO-66 ($Zr_6O_4(OH)_4(BDC)_6$), and MOF-5 ($Zn_4O(BDC)_3$). Such types of MOFS have received much attention in the research field because of their porosity, stability, and efficient applications.[111] MOFs can be prepared by using a variety of techniques such as hydrothermal, diffusion, microwave, mechanochemical, sonochemistry, and electrochemical techniques, as shown in Table 5 and Figure 5. In the hydrothermal approach, high temperature and pressure are utilized for the speedy preparation of MOFs.[112] In the case of the diffusion approach, ligands and metal ions are slowly mixed in a solvent to obtain MOF crystals over time. The microwave approach uses microwave irradiation to speed

https://doi.org/10.1021/acsomega.4c04532
ACS Omega 2024, 9, 34220−34242

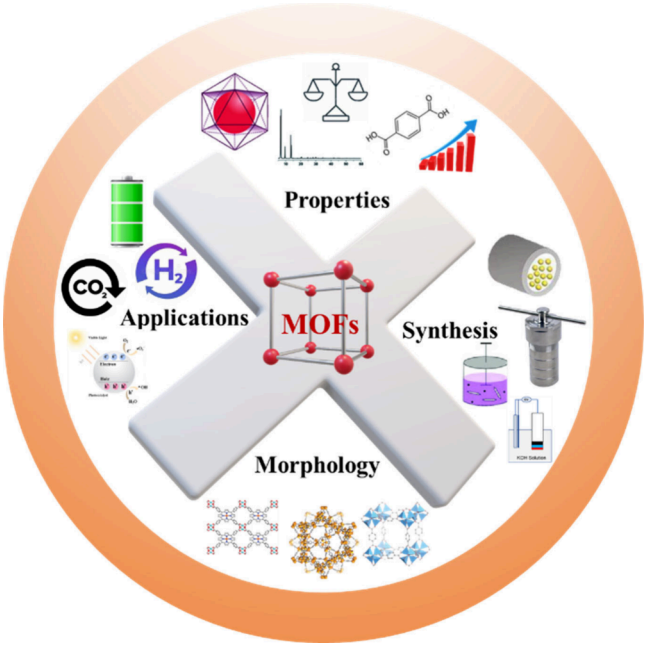

Figure 5. Overview of the applications, morphology, properties, and synthesis of MOFs.

up the reaction between ligands and metal ions.[113] The mechanochemical approach uses ball milling or grinding to perform reactions between ligands and metal ions.[114] Ultrasonic waves are used for the sonochemistry approach to accelerate the reaction and formation of MOFs. On the other hand, the electric current is utilized to form MOFs on conductive substrates in an electrochemical approach. MOFs offer a variety of applications in a wide range of fields because of their unique properties.[115] MOFs can act as heterogeneous catalysts in catalysis for various reactions, e.g., oxidation, CO_2 capture, CO_2 reduction, and hydrogenation.[116] Chen et al. constructed Fe-MOF with the acid regulator to improve the degradation.[117] Also, Xi et al. reported $CsPbBr_3$@2D-MOF as a photocatalyst for enhanced CO_2 reduction activity.[118] MOFs are useful for gas storage and separation applications because of their high surface area and variable pore size, which provide effective gas adsorption and separation.[119] In this regard, Ma and his team prepared a hierarchical porous MOF for enhanced uranium absorption.[120] MOFs also have great potential as sensors for detecting VOCs, gases, and heavy metals because of their high sensitivity and selectivity. Also, MOFs have been investigated for electrochemical charge storage applications, such as supercapacitors and batteries, due to their large surface area and capacity to accept guest species within their pores. Additionally, Xue et al. utilized MOFs in Zn metal batteries to improve long-term cycling and stability.[121] Likewise, MOFs demonstrate extraordinary structural diversity because there are so many different ways that organic ligands and metal ions can be combined.[122] This diversity allows researchers to create MOFs with required pore geometries, chemical functionalities, and pore sizes for desired applications. This ability to modify MOF structures opens new possibilities for tackling various challenges in several fields and continuing to be an active zone of research.[123]

7. COVALENT–ORGANIC FRAMEWORKS

COFs are a type of porous material that has been receiving tremendous attention in recent years because of its distinctive properties and applications.[107] The COF structure consists of organic building blocks that are linked by covalent bonding, resulting in a highly porous crystalline structure with high surface area, improved chemical stability, pore size tunability, and distinct functionality.[124] These properties make them a promising material for many applications like sensing, catalysis, electrochemical energy, and gas storage. COFs depend on the arrangement and connectivity of organic building blocks. COFs are categorized on the basis of their dimensions into 2D and 3D.[125] In 2D structures, the stacked layers of organic building blocks are held together by the help of weak interlayer interaction forces, which result in accessible pores and high surface areas, for example, imine-, triazine-, and boronate ester-linked COFs. While 3D COFs consist of interconnected 3D networks of covalent bands, e.g., imine, boronate ester, and amine linked, which leads to higher porosity and structural stability than 2D COFs.[126] COFs can be synthesized through various methods such as mechanochemical, hydrothermal, interfacial polymerization, microwave-assisted, and ionothermal under normal conditions, as shown in Table 6 and Figure 6. In the ionothermal approach, the ionic liquids are used as templates and solvents for COF synthesis. Generally, the reaction is carried out at high temperatures to form the covalent bonds between the organic building blocks.[127] The hydrothermal method consists of a reaction at high pressure and temperature which promotes the controlled growth of

Table 6. Examples of COFs and Their Applications

COF type	Synthesis method	Nature	Applications	Output	Ref.
2D keto-enamine-linked COF	Ionothermal	2D COF	Gas storage, catalysis, optoelectronics, and separation	High stability and surface area	127
TAPA-PMDA-COF, TAPB-PMDA-COF, TAPE-PMDA-COF, Py1P-COF	Hydrothermal	Imide-linked COF	Wide range such as photo- and electrocatalysts, etc.	High modularity	128
TH-COF	Microwave	Dioxin-linked COF	Microextraction	Reused 20 times, have high chemical and thermal stability	129
TpBD-COF	Mechanochemical	COF	Uranium removal	High reusability, adsorption rates, and capacity	130
Por-PD-COF	Condensation reaction	2D COF	Organic pollutant removal and gas separation	No photocatalytic and absorptive capacity lost after 4 times reused	133
XJCOF-1,2,3	Solvothermal	Zwitterionic COF	Ion conduction, catalysis and gas/molecular separation	High adsorption capacity and selectivity	134
TPB-DMTP-COF	Schiff base reaction	Benzoquinoline-linked COF	Li–S batteries and electrocatalytic O_2 reduction	High cycling durability and initial capacity	136

https://doi.org/10.1021/acsomega.4c04532
ACS Omega 2024, 9, 34220–34242

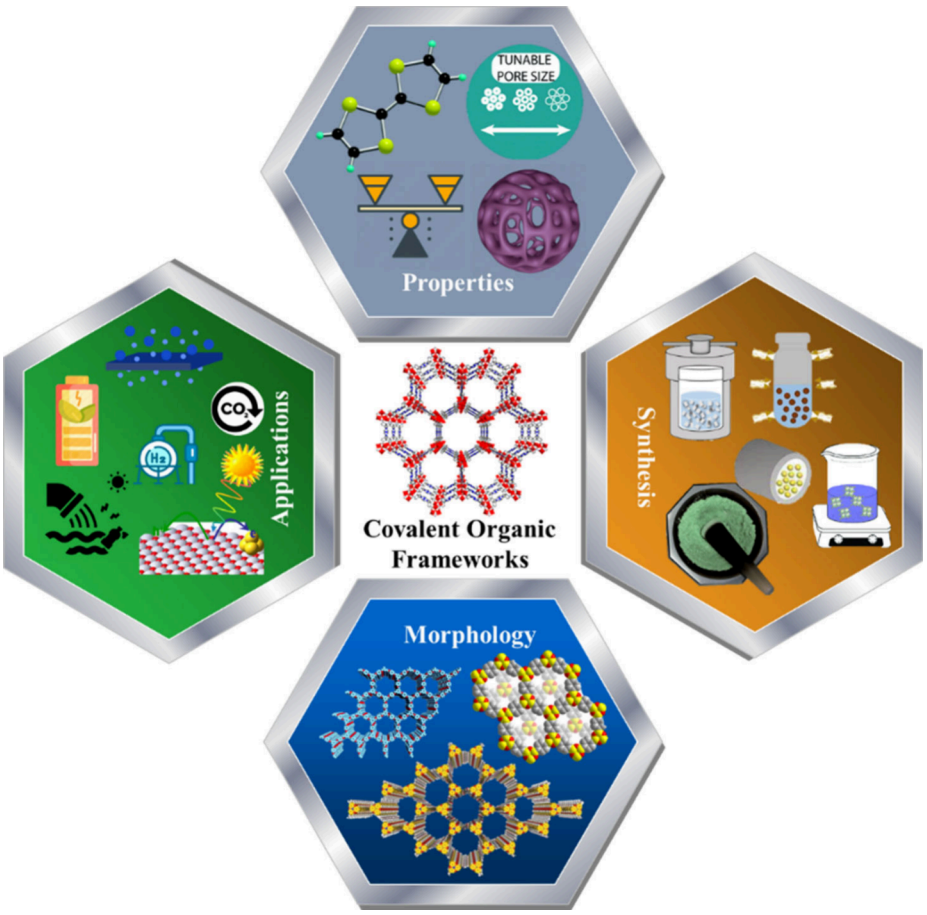

Figure 6. Overview of the applications, morphology, properties, and synthesis of the COFs.

crystals and covalent bond formations.[128] In the case of the microwave-assisted approach, microwave irradiation is used for heating which fastens the reaction and improves yield.[129] In the case of interfacial polymerization, the reaction is between two immiscible phases, generally liquid−solid or liquid−liquid. This technique is used for thin film formation on different substrates. Moving towards the mechanochemically scalable and simple approach that involves mechanical forces like ball milling or grinding under ambient conditions makes it useful on a commercial scale.[130] COFs have demonstrated large potential in a variety of applications, such as sensors, adsorption, catalysts, gas, and electrochemical charge storage, due to their unique properties. COFs can effectively work as heterogeneous catalysts in a lot of chemical reactions such as oxidation, photocatalysis, C−H activation, and hydrogenation due to their functional groups, tunable pore size, and large surface area.[131] The high porosity and surface area also enable COF usage in sensing applications such as chemical sensing, biosensing, and gas detection.[132] Very recently, Wu et al. designed and synthesized porphyrin-based COFs as photocatalysts and efficient adsorbents for organic pollutant degradation and specific molecule adsorption.[133] COFs are also explored for the adsorption and storage of gases such as CO_2, VOCs, and CH_4 due to their well-defined porous structure, which leads to their application in gas storage, separation, and carbon capture. Fu and his group utilized zwitterionic COFs for ion conduction and gas separation which showed high selectivity, adsorption capacity for SO_2/CO_2, and outstanding proton conductivity.[134] COFs can also be utilized for energy storage devices, e.g., batteries and supercapacitors as electrodes.[135] The high porosity and surface area of COFs provide many active sites for charge storage, and tunable electronic properties help to optimize the electrochemical performance. In this regard, Wu and co-workers utilized COFs for Li−S batteries and electrocatalytic O_2 reduction.[136] Moreover, COFs can improve the functionalities and properties of other materials when they are utilized as coatings or additives. The increasing amount of research in the characterization and synthesis of COFs can lead to unlocking its full potential for commercial applications.

8. HPS QDS@MOFS-COFS BASED MATERIALS

8.1. HPs QDs@MOFs. HPs QDs have emerged as promising materials for optoelectronic devices due to their excellent photophysical properties such as narrow emission line width, tunable bandgap, and high PLQY. However, their environmental sensitivity and stability are huge problems for large-scale applications. To overcome these challenges, researchers encapsulated HPs QDs within MOFs which give protection against heat, moisture, and oxygen. This serves as a key to the long-term performance of optoelectronic devices.[137] Furthermore, the high porosity of MOFs leads to improved diffusion and charge transport, which provides reduced recombination rates and enhanced charge carrier dynamics. There are also various synthesis techniques for the development of HPs QDs@MOFs. The most used method is the in situ growth of MOFs around already prepared HPs QDs. This approach generally involves the addition of the organic linkers

https://doi.org/10.1021/acsomega.4c04532
ACS Omega 2024, 9, 34220−34242

Table 7. Examples of HPs QDs@MOFs-COFs-Based Materials and Their Applications

HPs QDs@MOFs-COFs type	Synthesis method	Nature	Applications	Output	Ref.
$CsPbX_3$/MOF-5	In-situ growth in presynthesized MOF	HPs QDs/MOF	Optoelectronic	High photo and thermal stability	137
$MAPbBr_3$@UiO-66	In-situ	HPs QDs@MOF	Encryption/decryption	High PLQY and tunability	138
$CsPbBr_3$@PCN-333(Fe)	Sequential deposition approach	HPs QDs@MOF	Photocatalysis and cathodic	Improved cycling stability	140
$CsPbX_3$@MOF	In-situ growth in presynthesized MOF	HPs QDs@MOF	Displays, solar cells, photodetectors, and lasers	High PLQY and adsorption	141
$Cs_3Bi_2I_9$@NH_2-UiO-66	Postsynthesis	HPs QDs@MOF	Hydrogen production and light harvesting	High hydrogen production rate	142
$CH_3NH_3PbBr_3$ @ZIF-8	In a simple solution approach	HPs QDs@MOF	Sensors	High sensitivity and selectivity	143
$CsPbX_3$@ZIF-8	Postsynthesis	HPs QDs@MOF	Bright white LEDs	High stability	144
$CsPbX_3$@COF-SH	In-situ passivation	HPs QDs@COF	Optoelectronic	High operating stability and showed PLQY 81.5%	147
δ-$CsPbI_3$@TaPt-TP-COF	In-situ	HPs QDs@COF	PHE	High PHE rate and stability	148
$CsPbBr_3$@COF-V	Postsynthesis	HPs QDs@COF	Zn-air batteries and sensors	High output voltage (1.556 V) and performance	149
$CH_3NH_3PbBr_3$@COF	In-situ growth	HPs QDs@COF	LEDs	High water stability	150

and metal ions to HPs QDs containing solution and then controlled crystallization to prepare the MOF structure around HPs QDs.[138] Another approach is the coprecipitation of HPs QDs precursors, organic ligands, and metal ions in one solution which allows the simultaneous synthesis of HPs QDs and MOFs to prepare a well-defined hybrid.[139] Another approach is template-assisted growth in which preformed HPs QDs are embedded into presynthesized MOFs by chemical or physical methods.[140] The last one is postsynthetic encapsulation which involves the diffusion of HPs QDs into the preformed MOF pores in a suitable solvent. These techniques require careful control over reaction conditions like reaction time, solvent composition, and temperature to get the desired structure of hybrids.[141] MOFs/HPs QDs have shown their potential and flexibility in many applications such as sensor photocatalysis, decryption/encryption, water purification, adsorption, LEDs, storage, pollutant degradation, and solar cells. In photocatalysis, MOFs/HPs QDs have emerged as effective catalysts for several reactions due to their tunable bandgap and large surface area which allows them to effectively absorb light and produce charge carriers in photocatalytic reactions involving organic pollutant degradation, CO_2 conversion, and hydrogen generation through water splitting. Wang et al. prepared $Cs_3Bi_2I_9$(QDs)@NH_2-UiO-66 for enhanced photocatalytic hydrogen production and light harvesting.[142] As sensors, HPs QDs@MOFs offer high sensitivity and selectivity towards specific analytes due to strong fluorescence signals upon interaction with the target analyte, which is applied in the detection of various gases, heavy metals, and biomolecules. Very recently, a research team made a high-performance sensor by using $CH_3NH_3PbBr_3$(QDs)@ZIF-8 for monitoring aflatoxin.[143] Additionally, solar cells and LEDs benefit from the HPs QDs due to their excellent optoelectronic properties. In this regard, Zhao and his team utilized $CsPbX_3$(QDs)@ZIF-8 for bright white LEDs which demonstrated high stability.[144] These materials can be used as active layers in photovoltaic devices and light-emitting diodes to enhance their efficiency and performance. Significant progress has been made in understanding and utilizing HPs QDs@MOFs. However, there are undeniably many advanced applications that have yet to be discovered.[145]

8.2. HPs QDs@COFs. The development of HPs QDs@COFs has emerged as a promising area of research due to their exceptional properties and potential applications, as shown in Table 7 and Figure 7. COFs are highly ordered, crystalline porous materials composed of organic building blocks connected by covalent bonds. On the other hand, HPs QDs are nanoscale semiconductor crystals with excellent optoelectronic properties. The hybrid structure is formed by encapsulating HPs QDs within the pores or frameworks of COFs. This enhances the stability and performance of HPs

Figure 7. Overview of the applications, morphology, properties, and synthesis of HPs QDs@MOFs-COF-based materials.

https://doi.org/10.1021/acsomega.4c04532
ACS Omega 2024, 9, 34220−34242

Table 8. Examples of the HPs QDs@MOFs-COF-Based Material Applications

HPs QDs@MOFs-COFs type	Synthesis method	Nature	Applications	Output	Ref.
$CsPbBr_3$@Cu-TCPP	In-situ growth	HPs QDs@2D-COF	Photocatalytic CO_2 reduction	Improved electron−hole separation	151
$MAPbI_3$@PCN-221(Fe_x)	Post synthesis	HPs QDs@Fe based MOF	Photocatalytic CO_2 conversion and reduction	CH_4 and CO with 66% and 34% conversion rates	152
$MAPbBr_3$(QDs)@MA-$Mn(HCOO)_3$	Mechanochemical	HPs QDs@MOF	Photoelectrochemical activities	High stability	153
$CsPbBr_3$@ZIF-67	Facile in situ	HPs QDs@MOF	Photocatalytic CO_2 reduction	High catalytic activity	154
$Cs_2AgBiBr_6$@Ce-UiO-66-H	In-situ	LFHPs QDs@MOF	Photocatalytic CO_2 reduction and capturing	High reduction rates, stability, and nontoxicity	155
$CsPbBr_3/Cs_4PbBr_6$@COF	Simple solution based	HPs QDs@COF	Photocatalytic degradation	Recyclability up to six cycles	156
$CH_3NH_3PbBr_3$@MOF-5	Facile two-step	HPs QDs@MOF	Metal ion and temperature detection and future heavy metal remediation	High thermal and water stability	157
$CsPbX_3$@MOF	Facile two-step in situ growth	HPs QDs@MOF	Metal ion detection and future heavy metal remediation	High stability	158
$MAPb(Br/I)_3$, $MAPbCl_3$@Y346	Coprecipitation two-step in situ growth	HPs QDs@MOF	Photoredox catalysis and photocatalytic conversion	High stability	159
$MAPbBr_3$@TAPT-DMTA	In-situ	HPs QDs@COF	Wide future	Structural stability	160
$CsPbX_3$@AMOF-1	Mechanochemical postsynthesis	HPs QDs@MOF	Photovoltaic and optoelectronic	Good processability and stability	161
$CsPbBr_3$@ZIF-8	Mechanochemical	HPs QDs@MOF	Photocatalytic H_2 evolution	19.63 $\mu mol \cdot g^{-1}$ H_2 productivity in 2.5 h	162
Cs(Pb:Pt)Br_3 in Ni-MOF	Simple solution-based in situ growth	HPs QDs@MOF	Photocatalytic H_2 evolution	Good charge transfer and enhance photothermal stability	163
$MAPbBr_3$@UiO-66	In-situ growth	HPs QDs@Co-doped Ti-MOF	Photovoltaic and light-emitting	High PLQY of 43.3%	164
HP@Co-doped Ti-MOF	Solvothermal	HPs QDs@MOF	PSCs	High surface area and electron transport	165
$CsPbBr_3$@PCN-333(Fe)	Sequential deposition	HPs QDs@Fe based-MOF	Photoassisted Li−O_2 batteries and photocatalytic CO_2 reduction	Enhanced cycling stability	166
$CsPbX_3$@ZJU-28	In-situ growth	HPs QDs@MOF	Multifunctional applications like batteries, LEDs, etc	Better stability and optical properties	167
$CH_3NH_3PbBr_3$	Solution based	HPs QDs	Gas sensing	High PLQY	168
$MAPbBr_3$@In-pdda-1,2	In-situ growth	HPs QDs@MOF	Detection	Stable and tunable luminescence	169
$EDAPbCl_4$@ZIF-67	In-situ growth	HPs QDs@MOF	Electrochemical sensor	The detection limit of 15 μM	170
TpPa-1/Cs_2PdBr_6	Post synthesis	HPs QDs@2D-COF	NO_2 detection	High sensitivity and selectivity	171
$CsPbBr_3$/HZIF-8	In-situ growth	HPs QDs/MOF	Cu(II) detection	Good stability under UV light and moisture	172
$CsPbBr_3$@ZIF-8	Post synthesis	HPs QDs@MOF	NH_3 detection	High stability and sensitivity with a 16 ppm detection limit	173
HP@$[(TPA)_1(TPhT)_1]_{-C=N-}$	In-situ	HPs QDs@2D-COF	PSCs	Stability over 90%	174
$(FAPbI_3)_{0.83}(MAPbBr_3)_{0.17}(CsPbI_3)_{0.05}$@Car-ETTA	High-temperature solution based	HPs QDs@COF	PSCs	Efficiency up to 19.8%	175
HP@MOF-derived ZnO	Coordination reaction	MOF-derived ZnO-based PSCs	PSCs	Efficient electron extraction and light harvesting	176
$Cs_3Cu_2I_5$@MOF-74	Room temperature	LFHPs QDs@MOF	Optoelectronic	High stability and nontoxicity	177

QDs by preventing surface degradation and aggregation.[146] Also, they provide synergistic effects which lead to enhanced functionalities and properties. For the synthesis of COFs/HPs QDs, various methods are used for COF preparation, e.g., microwave-assisted, solvothermal, etc., and HPs QDs are prepared separately by solution-based techniques like the ligand-assisted or hot-injection approach. Finally, encapsulation is done by the postsynthetic method in which HPs QDs are added to a solution containing COFs and given time for HPs QDs to self-assemble in the COF structure. The second technique is in situ growth where precursors of COFs and HPs QDs are added in the same reaction mixture for simultaneous formation and growth of HPs QDs in COF structures.[147] COFs/HPs QDs have emerged as an efficient material for several applications such as catalysis, energy storage, and optoelectronics. Furthermore, HPs QDs improve the charge transfer, while the porosity of COFs gives a high surface area for catalytic reactions that make them appropriate for catalytic applications like electrocatalysis and photocatalysis. Notably, Yuan et al. prepared δ-$CsPbI_3$(QDs)@TaPt-TP-COF for PHE which showed a high PHE rate and stability.[148] HPs QDs@COFs also find applications in energy storage devices such as supercapacitors and batteries. As HPs QDs can improve charge storage and enhance device performance, on the other hand, the highly porous structure and large surface area of COFs increase the ion transport and energy storage capacity. Adding more, Xiao and co-workers synthesized $CsPbBr_3$(QDs)@COF-V and used it for Zn-air batteries in diagnostic sensors.[149] The unique optical properties of HPs QDs combined with the high surface area and stability of COFs make these hybrids promising materials for optoelectronic devices. They can be used in LEDs, photodetectors, and solar cells to enhance the device's performance and stability. In this regard, the researchers used $CH_3NH_3PbBr_3$(QDs)@COF for LEDs

https://doi.org/10.1021/acsomega.4c04532
ACS Omega 2024, 9, 34220−34242

which demonstrated improved water stability.[150] The unique combination of HPs QDs@COFs provides enhanced properties and stability, making them attractive materials for future technological advancements.

9. APPLICATIONS OF HPS QDS@MOFS-COF-BASED MATERIALS

This section highlights the potential applications of HPs QDs@MOFs-COF-based materials such as CO_2 conversion, hydrogen generation, gas sensing, pollutant degradation, batteries, and solar cells as shown in Table 8 and Figure 8.

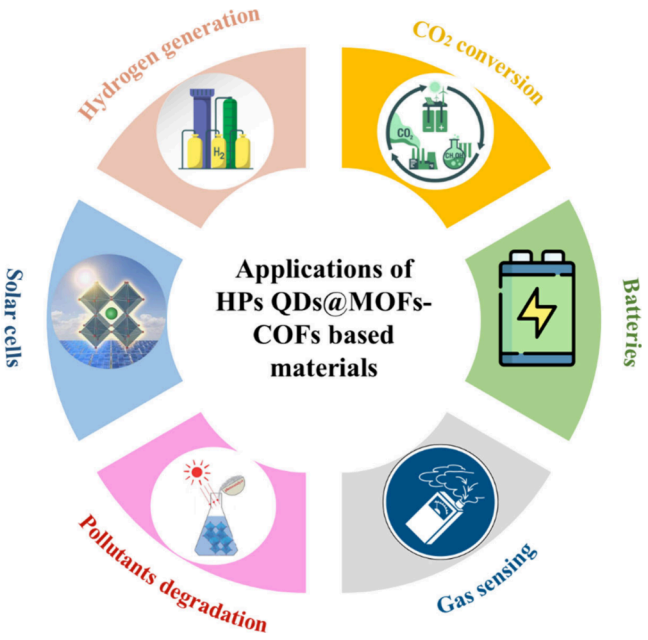

Figure 8. HPs QDs@MOFs-COFs-based materials applications.

9.1. CO_2 Conversion. CO_2 conversion is a crucial area of research and development aimed at mitigating climate change and utilizing carbon dioxide as a valuable resource.[178,179] However, perovskites are hardly reported for CO_2 conversion due to their instability and less active sites.[180] Coincidently, HPs QDs@MOFs-COFs hybrids are emerging as potential materials in various applications related to CO_2 conversion, including photocatalysis, electrochemical reduction, and CO_2 capture due to their efficient and sustainable approaches to addressing the global challenge of CO_2 emissions as shown in Figure 9.[181]

9.1.a. Photocatalytic CO_2 Conversion. One of the key applications of HPs QDs@MOFs-COFs hybrids in the CO_2 conversion is photocatalysis. These materials can act as efficient photocatalysts for the conversion of CO_2 into value-added chemicals or fuels using solar energy.[182] The HPs QDs@MOFs-COFs can absorb a broad range of solar radiation due to their tunable bandgaps, allowing for efficient light harvesting. The absorbed photons generate electron−hole pairs, which can then participate in various redox reactions to convert CO_2 into useful products such as CH_4, formate, or methanol.[183,184] The MOF or COF frameworks provide a stable and porous structure that facilitates the adsorption and activation of CO_2 molecules, enhancing the overall efficiency of the photocatalytic process. Notably, Zhang et al. prepared $CsPbBr_3$(QDs)@2D-Cu-TCPP with boosted electron−hole separation for photocatalytic CO_2 conversion and reduction.[151] Additionally, Wu and his research team synthesized the $MAPbI_3$(QDs)@PCN-221(Fe_x) photocatalyst and used it for CO_2 reduction to CH_4 and CO with 66% and 34% conversion rates.[152]

9.1.b. Electrochemical CO_2 Conversion. Another application of HPs QDs@MOFs-COFs hybrids in CO_2 conversion is electrochemical reduction. These hybrid materials can be used as catalysts in electrochemical cells to convert CO_2 into valuable chemicals or fuels using electricity as an energy source.[185] The HPs QDs@MOFs-COFs can serve as efficient electrocatalysts due to their high surface area, abundant active sites, and excellent charge transport properties. The structure of COFs or MOFs gives conductivity and stability, which allows the activation and adsorption of CO_2 molecules, improving the electrochemical reduction. Products like CO, ethylene, and formic acid can be synthesized by carefully controlling the structure and composition of hybrids. Notably, a team of researchers manufactured MA-Mn$(HCOO)_3$/$MAPbBr_3$(QDs) and utilized them for photoelectrochemical activities with improved stability.[153]

9.1.c. CO_2 Capture. In addition to CO_2 conversion, HPs QDs@MOFs-COFs hybrids can also be utilized for CO_2 capture. These materials can selectively adsorb CO_2 from flue gas or other emission sources, enabling its efficient capture and subsequent storage or utilization. The porous structures of MOFs and COFs provide a large surface area and high

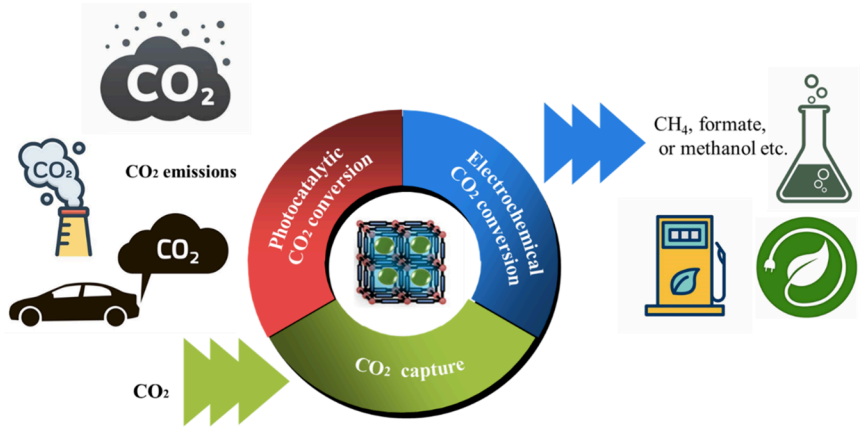

Figure 9. Schematic diagram of photocatalytic, electrochemical CO_2 conversion, and CO_2 capture through HPs QDs@MOFs-COFs hybrids.

https://doi.org/10.1021/acsomega.4c04532
ACS Omega 2024, 9, 34220−34242

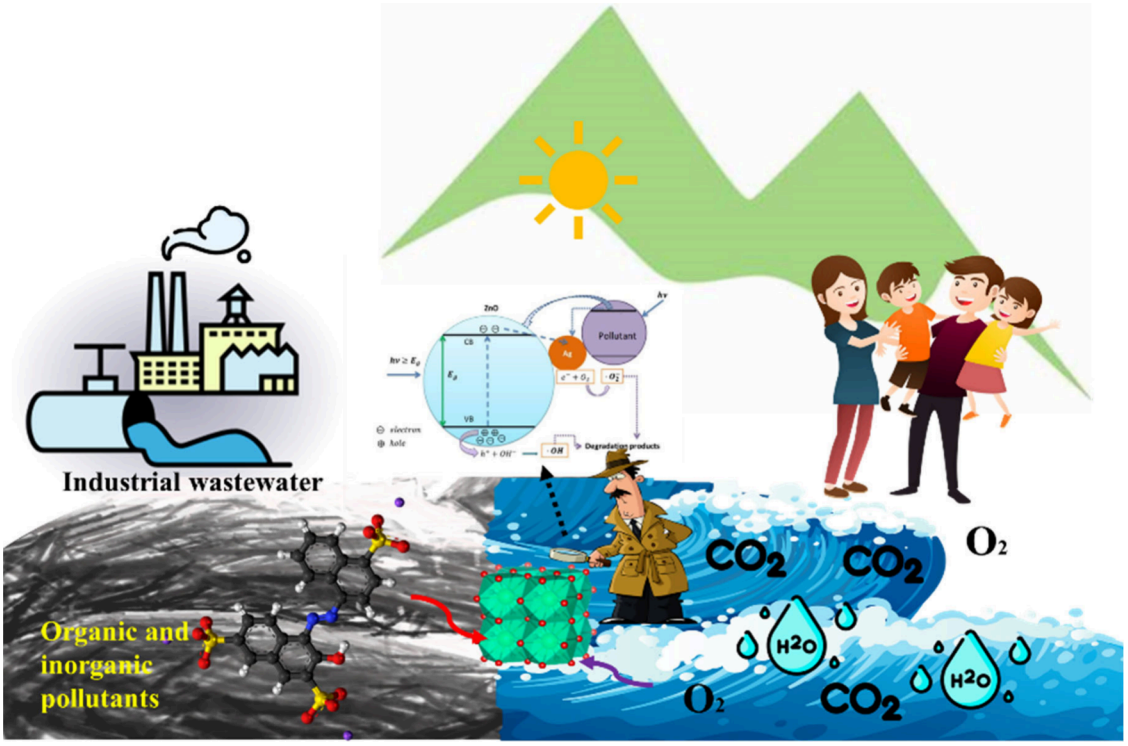

Figure 10. Schematic diagram of pollutant degradation through HPs QDs@MOFs-COFs hybrids.

adsorption capacity, allowing for the effective capture of CO_2 molecules. HPs QDs embedded within the frameworks can further enhance the CO_2 capture performance by providing additional adsorption sites and facilitating the diffusion of the CO_2 molecules within the materials. The captured CO_2 can then be released through thermal or pressure swing desorption for further utilization or sequestration.[154] Ding et al. prepared $Cs_2AgBiBr_6$(QDs)@Ce-UiO-66-H for outstanding photocatalytic CO_2 reduction and capturing.[155]

9.2. Pollutant Degradation. Pollutant degradation is very needed nowadays to mitigate the harmful effects of pollutants on human health, ecosystems, and the environment.[186,187] To overcome these shortcomings, HPs QDs@MOFs-COFs hybrids have demonstrated great potential in the degradation of both organic and inorganic pollutants.[188,189] Their unique combination of MOFs or COFs with HPs QDs allows for synergistic effects that enhance pollutant degradation through mechanisms such as photocatalysis, adsorption, oxidation, and ion exchange, as shown in Figure 10.

9.2.a. Organic Pollutants. HPs QDs@MOFs-COFs have been extensively studied for the degradation of various organic pollutants.[190] These materials can effectively degrade organic pollutants through different mechanisms such as photocatalysis, adsorption, and oxidation.[191] In photocatalysis, these hybrid materials can act as efficient photocatalysts under visible light irradiation.[192] HPs QDs exhibit strong absorption in the visible range, allowing them to generate electron−hole pairs upon light excitation. These charge carriers can then react with organic pollutants adsorbed on the surface of MOFs or COFs, leading to their degradation into harmless byproducts. Moreover, MOFs and COFs possess high surface areas and well-defined pore structures, which make them excellent adsorbents for organic pollutants. By encapsulation of HPs QDs within these frameworks, the hybrid materials can combine the adsorption capacity of MOFs or COFs with the photocatalytic activity of QDs. This synergistic effect enhances the removal efficiency of organic pollutants from contaminated water or air.[193] HPs QDs@MOFs-COFs can also promote the oxidation of organic pollutants through the generation of ROS. Under light irradiation, the excited QDs can transfer electrons to molecular oxygen, producing ROS such as hydroxyl radicals (•OH) or superoxide radicals.[194] These ROS are highly reactive and can effectively oxidize organic pollutants, breaking them down into less harmful substances. Notably, Kour et al. used $CsPbBr_3/Cs_4PbBr_6$@COF for photocatalytic methyl orange degradation which demonstrated enhanced recyclability for up to six cycles.[156]

9.2.b. Inorganic Pollutants. In addition to organic pollutants, HPs QDs@MOFs-COFs have also shown promise in the degradation of various inorganic pollutants. The unique properties of these hybrid materials enabling them to efficiently remove and degrade inorganic pollutants through different mechanisms.[157] Similar to the degradation of organic pollutants, the photocatalytic activity of hybrid materials can be harnessed for the degradation of inorganic pollutants.[195] Under light irradiation, HPs QDs@MOFs-COFs generate charge carriers that can react with inorganic pollutants, leading to their degradation or transformation to less toxic forms. MOFs and COFs have been widely studied for their adsorption capabilities towards inorganic pollutants. By encapsulating HPs QDs within MOFs−COFs frameworks, the hybrid materials can combine the high adsorption capacity of MOFs or COFs with the photocatalytic activity of QDs. This allows for the efficient removal and degradation of inorganic pollutants from contaminated environments.[196] Moreover, some MOFs and COFs possess ion exchange properties, which can be utilized for the removal of specific inorganic pollutants.[197] By incorporation into these frameworks, the hybrid materials can enhance their ion exchange capabilities and improve the removal efficiency of targeted

https://doi.org/10.1021/acsomega.4c04532
ACS Omega 2024, 9, 34220−34242

inorganic pollutants. Very recently, Ahmed et al. prepared $CsPbX_3$(QDs)@MOF for metal ion detection and future heavy metal remediation, which showed good stability.[158]

9.3. Hydrogen Generation. Hydrogen gas is considered a clean and renewable energy carrier, as it can be produced from various sources such as water, biomass, or even waste materials.[198,199] However, the current methods for hydrogen production often rely on fossil fuels or expensive noble metal catalysts, which are not sustainable or cost-effective in the long run.[200] Thus, it is the need of the hour to develop alternative catalysis that can help in hydrogen production from inexpensive and abundant resources.[201] In this regard, HPs QDs@MOFs-COFs have been seen as an effective hydrogen production approach, as shown in Figure 11. HPs QDs are

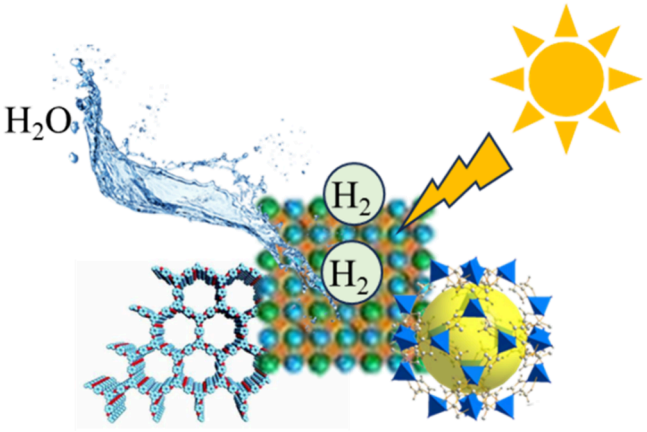

Figure 11. Schematic diagram of hydrogen generation through HPs QDs@MOFs-COFs-based materials.

semiconductor nanocrystals with unique optoelectronic properties, and encapsulating them within COFs-MOFs makes them more stable and enhances their catalytic activity. HPs QDs@MOFs-COFs provide various benefits in hydrogen generation.[159] For example, the COFs-MOFs porous structure gives abundant active sites and high surface area for catalytic reactions that lead to the efficient activation and adsorption of reactant molecules involved in hydrogen production. Second, COFs-MOFs protect HPs QDs from degradation and improve stability under harsh conditions. Likewise, HP QD properties, such as high absorption coefficient and tunable bandgap, facilitate effective light harvesting for use in photocatalytic hydrogen production. So, HPs QDs@MOFs-COFs show improved charge transport and light absorption leading to enhanced photocatalysis and overall high hydrogen generation.[160] Hydrogen generation through HPs QDs@MOFs-COFs can be done by several approaches depending on the experimental conditions and specific materials. One of the common pathways is photocatalytic water splitting in which absorbed photos produce electron−hole pairs in HP QDs. These charge carriers are then transferred to MOFs-COFs, where they take part in redox reactions with H_2O molecules to produce H_2 gas.[161] Another feasible pathway involves the activation of small molecules like formic acid or alcohols that can work as a H_2 source. The MOF/COF catalysts can facilitate the dehydrogenation reactions of these molecules, releasing hydrogen gas as a byproduct. The encapsulated HPs QDs can enhance the catalytic activity by promoting charge transfer and facilitating the regeneration of active sites within the MOF/COF matrices. Notably, a group of researchers showed HP QDs@MOF ability for clean energy production and LEDs.[202] Feng and his co-workers prepared photocatalyst $CsPbBr_3$@ZIF-8 for hydrogen evolution, which demonstrated 19.63 $\mu mol \cdot g^{-1}$ H_2 productivity in 2.5 h.[162] Moreover, Zhang et al. confined Cs(Pb: Pt)Br_3 QDs in Ni-MOF pores to overcome the poor charge transfer and enhance photothermal stability to get higher hydrogen production.[163] Further research and development in this field are needed to optimize the design and synthesis of MOF/COF encapsulated HPs QDs for practical applications in sustainable hydrogen production.

9.4. Batteries. HP QDs@MOFs-COFs have shown great potential in the field of batteries. This hybrid material offers several advantages that can enhance the performance and efficiency of batteries, as shown in Figure 12. One of the HPs

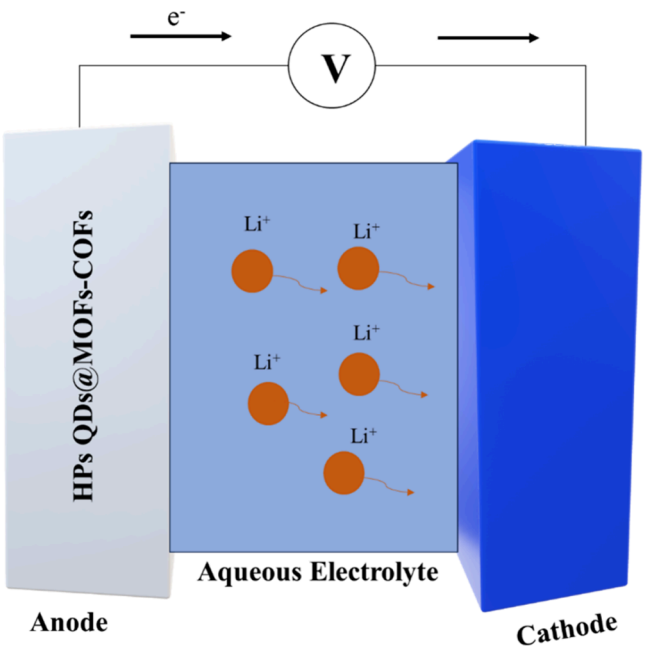

Figure 12. Schematic diagram of a battery consisting of HPs QDs@MOFs-COFs-based materials.

QDs@MOFs-COFs applications is in the field of batteries due to COFs-MOFs providing a large surface area for the deposition of HPs QDs, allowing more active material loading in the battery that increases energy storage capacity.[164] Moreover, the large surface area provides efficient ion diffusion and electrolyte penetration, followed by enhanced charge/discharge rates. HPs QDs@MOFs-COFs also improve the cycling performance and stability of batteries by preventing degradation under harsh conditions like oxygen, heat, and moisture.[165] Additionally, the use of LFHPs QDs can also enhance the safety of batteries. In this regard, Qiao et al. prepared $CsPbBr_3$(QDs)@PCN-333(Fe) to improve the stability of photoassisted lithium oxide batteries with enhanced cycling stability.[166] Ren and his team synthesized $CsPbX_3$(QDs)@ZJU-28 for multifunctional applications like batteries, LEDs, etc., with better stability and optical properties.[167] For solar cells or batteries, lead-based HPs materials are widely studied due to their better efficiency but are toxic to the environment. Thus, toxicity can be eliminated by using LFHPs QDs. Lastly, these materials have the potential

https://doi.org/10.1021/acsomega.4c04532
ACS Omega 2024, 9, 34220−34242

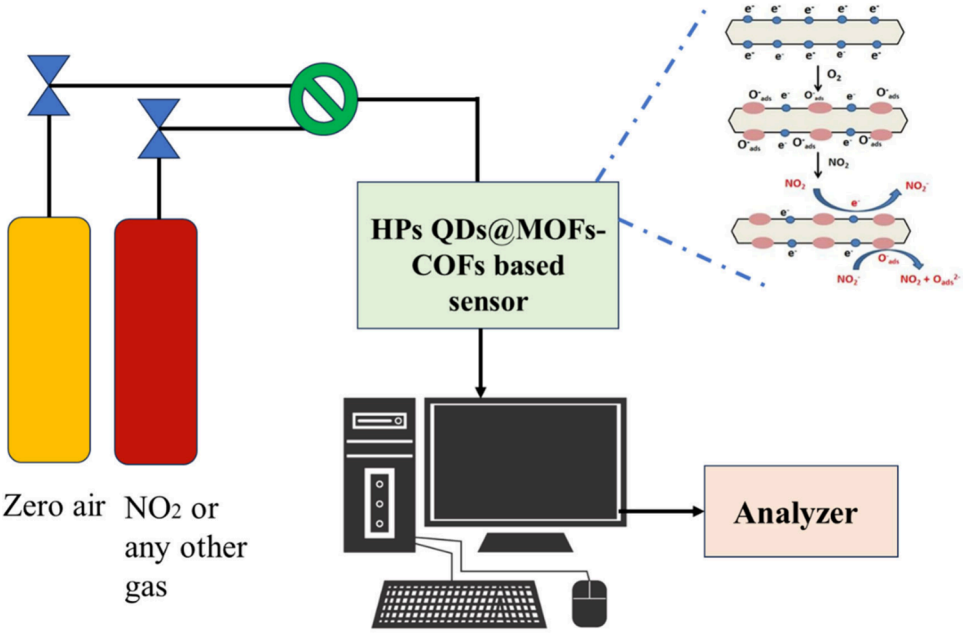

Figure 13. Schematic diagram of gas sensing through HPs QDs@MOFs-COFs-based materials.

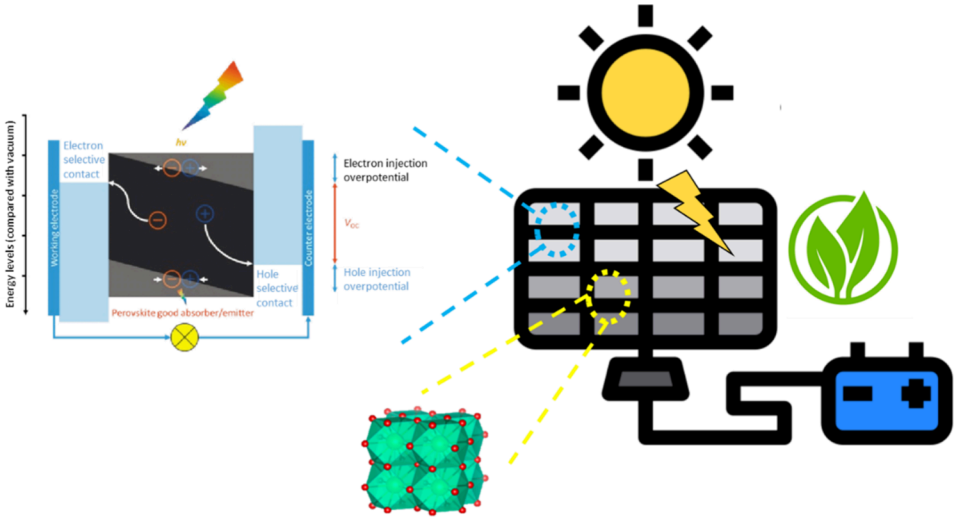

Figure 14. Schematic diagram of the solar cell consisting of HPs QDs@MOFs-COFs-based materials.

to revolutionize the field of battery technology by addressing key challenges and improving the overall performance.

9.5. Gas Sensing. Gas sensing is a crucial technology used for detecting and monitoring the presence of various gases in the environment. It finds applications in diverse fields such as industrial safety, environmental monitoring, healthcare, and homeland security. The ability to accurately detect and quantify different gases is essential for ensuring human safety and environmental protection. Despite the great potential of HP QDs as sensing materials, researchers are still dealing with the stability and water resistance challenges in this field. Singh et al. prepared $CH_3NH_3PbBr_3$(QDs) for gas sensing, but they demonstrated instability and decreased PL intensity in the presence of NH_3.[168] That is why encapsulating HPs QDs within MOFs or COFs has emerged as a novel approach to enhance the performance of gas sensors. The combination of HPs QDs with MOFs or COFs offers several advantages, including improved stability, enhanced optical properties, and increased surface area for gas adsorption.[169] This hybrid material system has shown huge potential for gas-sensing applications, particularly in the detection of toxic gases, environmental pollutants, and VOCs as shown in Figure 13. One example of the application of HPs QDs@MOFs-COFs in gas sensing is the detection of the oxide boron ligands of NO_2. NO_2 is a highly toxic gas that is primarily emitted from vehicle exhaust and industrial processes, causes respiratory problems, and contributes to air pollution. Conventional NO_2 sensors or detectors frequently suffer from low selectivity and sensitivity.[170] However, gas sensor performance can be improved by using LFHPs and QDS@MOFs-COFs. HPs QDs can perform as effective electron acceptors that improve the charge transport between the sensing material and the target gas molecules. This allows higher selectivity and sensitivity towards NO_2 detection. Additionally, a group of researchers prepared TpPa-1(2D-COF)/Cs_2PdBr_6 for NO_2 detection with high sensitivity and selectivity.[171] The detection of VOCs is also an

https://doi.org/10.1021/acsomega.4c04532
ACS Omega 2024, 9, 34220−34242

example of gas sensing. VOCs are organic chemicals that can easily vaporize at ambient temperature, are mostly found indoors, and have harmful effects on human health. HPs QDs@MOFs-COFs have demonstrated great potential in VOC detection, e.g., benzene, toluene, and formaldehyde. HPs QDs provide efficient optical properties for signal transduction, while COFs/MOFs provide many active sites for gas absorption due to their porosity and large surface area. In return, this increases the selective and sensitive detection of VOCs at low concentrations.[172] Moreover, HPs QDs@MOFs-COFs can also be used for the detection of other gases such as H_2S, CH_4, CO_2, and NH_3. In this regard, Ahmad et al. synthesized $CsPbBr_3$(QDs)@ZIF-8 for NH_3 detection which displayed high stability and sensitivity at ambient conditions with a 16 ppm detection limit.[173] Every gas has its own unique properties and poses several challenges for sensing. However, by modification of the structure and composition of sensing materials, it is possible to make gas sensors with high specificity and performance for different target gases.

9.6. Perovskite Solar Cells. The need for LFHPs QDs@MOFs-COFs in the field of solar cells is rising due to the quest to overcome the challenges related to lead-based PSCs.[203] LFHPs QDs@MOFs-COFs materials can also enhance the performance of PSCs by improving their stability, versatility, and efficiency of solar cells. One of the key pros of utilizing HPs QDs@MOFs-COFs in solar cells is their capability to improve light absorption. HPs QDs exhibit efficient absorption in visible light, as 50% of sunlight is visible. On the other hand, COF/MOF porous structure and high surface area give a large interface for QD deposition which leads to effective light harvesting. Figure 14 demonstrates the improved photocurrent generation and light absorption in solar cells achieved by the resulting hybrid.[204] Moreover, COFs or MOFs also work as hole transport layers (HTLs) or as electron transport layers (ETLs) in solar cells, which play an important role in effective charge transport and separation. This led to enhanced device performance and electronic properties such as high hole mobility or electron affinity.[174] COFs/MOFs also provide stability to HPs QDs against oxygen and moisture, preventing their degradation and providing effective charge transport. Other than enhancing the stability and performance of solar cells, COFs or MOFs are also used in the fabrication of transparent and flexible devices such as building-integrated photovoltaics and flexible electronics. By integrating COFs or MOFs into the structure of the device, it is possible to achieve bendable, semitransparent, and lightweight solar cells. Notably, a team of researchers synthesized $(FAPbI_3)_{0.83}(MAPbBr_3)_{0.17}(CsPbI_3)_{0.05}$-based PSCs by using Car-ETTA(COF) which showed efficiency up to 19.8%.[175] Also, Zhang and his co-workers prepared MOF-derived ZnO-based PSCs with efficient electron extraction and light harvesting.[176] LFHPs QDs@MOFs-COFs materials offer improved stability, lower toxicity, and enhanced environmental sustainability, making them a promising avenue for the future development of efficient and eco-friendly solar energy technologies. Zhang et al. confined $Cs_3Cu_2I_5$(QDs) in MOF-74 for optoelectronic applications with high stability and nontoxicity.[177] Further research and development in this field are expected to unlock the full potential of HPs QDs@MOFs-COFs in solar cell applications.

10. CONCLUSION

Perovskites are revolutionary materials, and their potential lies in numerous industries as they have cost-effective synthesis and versatility with good properties. Still, these materials have some limitations and environmental issues that the structure can address. and coupling/encapsulating with other materials like COFs or MOFs because MOFs or COFs have simple preparation, high chemical/thermal stability, large surface area, and low density. In this review, we summarized the importance, properties, morphology, synthesis, and applications of perovskites, HPs, LFHPs, HPs QDs, MOFs, COFs, and HPs QDs@MOFs-COFs-based materials. After providing a comprehensive overview, some potential applications of HP QDs@MOFs-COFs-based materials in the fields of CO_2 conversion, pollutant degradation, hydrogen generation, batteries, gas sensing, and solar cells are discussed. Finally, some current trends, future outlooks, and challenges regarding QDs@MOFs-COFs-based materials and their applications are discussed. Moreover, HP QDs@MOF-COFs are most competitive with state-of-the-art materials due to their adjustable optoelectronic characteristics and potential for cost-effective manufacture in fields including LEDs, photovoltaics, sensors, and catalysis. LFHP QDs@MOF-COF research is anticipated to advance in the upcoming years because of developments in material design, synthesis methods, and knowledge of structure−property connections. Advancements focused on augmenting stability, optimizing efficacy, and diminishing toxicity are anticipated to facilitate the expansion of these materials' uses in diverse sectors.

■ ASSOCIATED CONTENT

Data Availability Statement

The data underlying in this study are available in the published article and its Supporting Information.

■ AUTHOR INFORMATION

Corresponding Author

Iltaf Khan − *School of Environmental & Chemical Engineering, Jiangsu University of Science and Technology, Zhenjiang 212100, China;* orcid.org/0000-0001-8045-697X; Email: doctoriltafkhan@just.edu.cn

Authors

Anam Altaf − *School of Environmental & Chemical Engineering, Jiangsu University of Science and Technology, Zhenjiang 212100, China*

Aftab Khan − *College of Material Science and Engineering, Beijing University of Chemical Technology, Beijing 100029, China*

Samreen Sadiq − *Jiangsu Key Laboratory of Sericultural and Animal Biotechnology, School of Biotechnology, Jiangsu University of Science and Technology, Zhenjiang 212100, China*

Muhammad Humayun − *Energy, Water, and Environment Lab, College of Humanities and Sciences, Prince Sultan University, Riyadh 11586, Saudi Arabia;* orcid.org/0000-0003-3504-3935

Shoaib Khan − *College of Horticulture and Landscape Architecture, Northeast Agricultural University, Harbin 150030, China*

Saeed Zaman − *College of Chemistry, Liaoning University, Shenyang 110036, China*

https://doi.org/10.1021/acsomega.4c04532
ACS Omega 2024, 9, 34220−34242

Abbas Khan − *Energy, Water, and Environment Lab, College of Humanities and Sciences, Prince Sultan University, Riyadh 11586, Saudi Arabia; Department of Chemistry, Abdul Wali Khan University, Mardan 23200, Pakistan;* orcid.org/0000-0002-2882-8761

Rasha A. Abumousa − *Energy, Water, and Environment Lab, College of Humanities and Sciences, Prince Sultan University, Riyadh 11586, Saudi Arabia;* orcid.org/0000-0002-0712-9662

Mohamed Bououdina − *Energy, Water, and Environment Lab, College of Humanities and Sciences, Prince Sultan University, Riyadh 11586, Saudi Arabia*

Complete contact information is available at: https://pubs.acs.org/10.1021/acsomega.4c04532

Author Contributions

●A.A., A.K., and S.S. contributed equally. Anam Altaf: Writing - original draft, Writing - review and editing. Iltaf Khan: Writing - original draft, Investigation, Conceptualization, Resources, Supervision. Aftab Khan: Writing - original draft, Writing - review and editing. Samreen Sadiq: Writing - original draft, Writing - review and editing. Muhammad Humayun: Methodology, Conceptualization, Resources, Supervision. Shoaib Khan: Formal analysis, Software. Saeed Zaman: Methodology, Conceptualization, Resources. Abbas Khan: Validation, Data curation, Writing - review and editing. Rasha A. Abumousa: Formal analysis, Software. Mohamed Bououdina: Validation, Data curation.

Notes

The authors declare no competing financial interest.

■ ACKNOWLEDGMENTS

The authors are grateful and would like to thank Jiangsu University of Science and Technology (Grant No. 1112932205) for financial support. The authors are grateful and would like to thank Prince Sultan University Riyadh for paying the Article Processing Charges (APC).

■ ABBREVIATIONS AND LIST OF ACRONYMS

1D	One-dimensional
2D	Two-dimensional
3D	Three-dimensional
ALD	Atomic layer deposition
COFs	Covalent−organic frameworks
CVD	Chemical vapor deposition
ETLs	Electron transport layers
HPs	Halide perovskites
HPs QDs	Halide perovskite quantum dots
HTLs	Hole transport layers
LEDs	Light emitting diodes
LFHPs	Lead-free halide perovskites
MOFs	Metal−organic frameworks
PCBs	Polychlorinated biphenyls
PCEs	Power conversion efficiencies
PHE	Photocatalytic hydrogen evolution
PL	Pillared layered
PLQY	Photoluminescence quantum yield
POPs	Persistent organic pollutants
PSCs	Perovskite solar cells
ROS	Reactive oxygen species
UiO	University of Oslo
VOCs	Volatile organic compounds
ZIFs	Zeolitic imidazolate frameworks

■ REFERENCES

(1) Zaman, S.; et al. Synthesis of mediator free hollow BiFeO3 spheres/porous g-C3N4 Z-scheme photocatalysts for CO2 conversion and Alizarin Red S degradation. *Materials Science in Semiconductor Processing* **2023**, *162*, No. 107534.

(2) Khan, I.; et al. Biological Inspired Green Synthesis of TiO2 Coupled g-C3N4 Nanocomposites and Its Improved Activities for Sulfadiazine and Bisphenol A Degradation. *Journal of Cluster Science* **2023**, *34* (3), 1453−1464.

(3) Chen, Z.-K.; et al. Sensitive NO detection by lead-free halide Cs2TeI6 perovskite with Te-N bonding. *Sens. Actuators, B* **2022**, *357*, No. 131397.

(4) Israr, M. Multi-metallic electrocatalysts as emerging class of materials: opportunities and challenges in the synthesis, characterization, and applications. *Catalysis Reviews* **2024**, 1−61.

(5) Asghar, H.; et al. Synthesis of g-C3N4/SmFeO3 nanosheets Z-scheme based nanocomposites as efficient visible light photocatalysts for CO2 reduction and Congo red degradation. *J. Mater. Res.* **2023**, *38* (11), 2986−2997.

(6) Elfatouaki, F.; et al. Optoelectronic and thermoelectric properties of double halide perovskite Cs2AgBiI6 for renewable energy devices. *Sol. Energy* **2023**, *260*, 1−10.

(7) Huang, S.; et al. Molecularly imprinted mesoporous silica embedded with perovskite CsPbBr3 quantum dots for the fluorescence sensing of 2,2-dichlorovinyl dimethyl phosphate. *Sens. Actuators, B* **2020**, *325*, No. 128751.

(8) Zhang, Y.; et al. Molecular-functionalized metal-organic frameworks enabling contact-electro-catalytic organic decomposition. *Nano Energy* **2023**, *111*, No. 108433.

(9) Ge, Y.; et al. Tuning the structure characteristic of the flexible covalent organic framework (COF) meets a high performance for lithium-sulfur batteries. *Nano Energy* **2023**, *109*, No. 108297.

(10) Younes, H. A.; et al. Perovskite/metal-organic framework photocatalyst: A novel nominee for eco-friendly uptake of pharmaceuticals from wastewater. *J. Alloys Compd.* **2023**, *930*, No. 167322.

(11) Wang, P.; et al. Direct Z-scheme heterojunction of PCN-222/CsPbBr3 for boosting photocatalytic CO2 reduction to HCOOH. *Chem. Eng. J.* **2023**, *457*, No. 141248.

(12) Nisar, A.; et al. Kinetic modeling of ZnO-rGO catalyzed degradation of methylene blue. *Int J of Chemical Kinetics* **2020**, *52* (10), 645−654.

(13) Sadiq, S. Recent Updates on Multifunctional Nanomaterials as Antipathogens in Humans and Livestock: Classification, Application, Mode of Action, and Challenges. *Molecules* **2023**, *28*, 7674.

(14) Meng, G.; et al. Confining perovskite quantum dots in the pores of a covalent-organic framework: quantum confinement- and passivation-enhanced light-harvesting and photocatalysis. *Journal of Materials Chemistry A* **2021**, *9* (43), 24365−24373.

(15) Liu, T.; et al. A visual electrochemiluminescence molecularly imprinted sensor with Ag+@UiO-66-NH2 decorated CsPbBr3 perovskite based on smartphone for point-of-care detection of nitrofurazone. *Chem. Eng. J.* **2022**, *429*, No. 132462.

(16) Xiang, X.; et al. Preparation of CH3NH3PbBr3 Perovskites Encapsulated in ZIF-8 with Improved Stability and Their Application in Fluorimetry and Information Encryption. *Langmuir* **2023**, *39* (15), 5315−5322.

(17) Li, J.; et al. Processing bulk insulating CaTiO3 into a high-performance thermoelectric material. *Chem. Eng. J.* **2022**, *428*, No. 131121.

(18) Yaseen, W. Facile synthesis of CoMoO4/CoMoB/boron-doped carbon nanocomposite as a highly durable bifunctional electrocatalyst for overall water splitting. *Int. J. Hydrogen Energy* **2024**, *51*, 565.

(19) Ehsan, M. F.; et al. CoFe2O4 decorated g-C3N4 nanosheets: New insights into superoxide anion mediated photomineralization of methylene blue. *Journal of Environmental Chemical Engineering* **2020**, *8* (6), No. 104556.

(20) Khan, I.; et al. Improved visible-light photoactivities of porous LaFeO3 by coupling with nanosized alkaline earth metal oxides and mechanism insight. *Catalysis Science & Technology* **2019**, *9* (12), 3149−3157.
(21) Hussain, S.; et al. Influence of rare earth ions (Dy3+, Eu3+, La3+) on the ultraviolet-light photocatalytic activity and magnetic properties of BiFeO3. *Mater. Chem. Phys.* **2022**, *290*, No. 126581.
(22) Sabir, M.; et al. Rare earth and transition metal co-doped LaFeO3 perovskite and its CNTs reinforced nanohybrid for environmental remediation application. *Ceram. Int.* **2023**, *49* (12), 20939−20950.
(23) Khan, I. Efficient CO2 conversion and organic pollutants degradation over Sm3+ doped and rutile TiO2 nanorods decorated-GdFeO3 nanorods. *Int. J. Hydrogen Energy* **2023**, *48*, 32756.
(24) Chang, H.; et al. Polyarylimide-Based COF/MOF Nanoparticle Hybrids for CO2 Conversion, Hydrogen Generation, and Organic Pollutant Degradation. *ACS Appl. Nano Mater.* **2024**, *7* (9), 10451−10465.
(25) Wang, X. Immobilization of Horseradish Peroxidase and Myoglobin Using Sodium Alginate for Treating Organic Pollutants. *Water* **2024**, *16*, 848.
(26) Park, J. K.; et al. Synthesis of post-processable metal halide perovskite nanocrystals via modified ligand-assisted re-precipitation method and their applications to self-powered panchromatic photo-detectors. *Journal of Industrial and Engineering Chemistry* **2020**, *92*, 167−173.
(27) Cernea, M.; et al. Preparation by sol−gel and solid state reaction methods and properties investigation of double perovskite Sr2FeMoO6. *J. Eur. Ceram. Soc.* **2013**, *33* (13), 2483−2490.
(28) Luo, X.; et al. Mechanochemical synthesis of La-Sr-Co perovskite composites for catalytic degradation of doxycycline in the dark: Role of oxygen vacancies. *Sep. Purif. Technol.* **2022**, *300*, No. 121891.
(29) Ngqoloda, S.; et al. Mixed-halide perovskites solar cells through PbICl and PbCl2 precursor films by sequential chemical vapor deposition. *Sol. Energy* **2021**, *215*, 179−188.
(30) Li, W.; et al. Enhancing the electrocatalytic activity of perovskite electrodes by atomic layer-deposited doped CeO2 for symmetrical solid oxide fuel cells. *Sep. Purif. Technol.* **2022**, *302*, No. 122135.
(31) Tan, S.; et al. Temperature-Reliable Low-Dimensional Perovskites Passivated Black-Phase CsPbI3 toward Stable and Efficient Photovoltaics. *Angew Chem Int Ed* **2022**, *61* (23), No. e202201300.
(32) Lin, R.; et al. All-perovskite tandem solar cells with improved grain surface passivation. *Nature* **2022**, *603* (7899), 73−78.
(33) Khan, I.; et al. Synthesis of SnO2/yolk-shell LaFeO3 nanocomposites as efficient visible-light photocatalysts for 2,4-dichlorophenol degradation. *Mater. Res. Bull.* **2020**, *127*, No. 110857.
(34) Qin, W.; et al. Phosphorus-doped porous perovskite LaFe1-xPxO3-δ nanosheets with rich surface oxygen vacancies for ppb level acetone sensing at low temperature. *Chem. Eng. J.* **2022**, *431*, No. 134280.
(35) Tian, K.; et al. Design and fabrication of spinel nanocomposites derived from perovskite hydroxides as gas sensing layer for volatile organic compounds detection. *Sens. Actuators, B* **2021**, *329*, No. 129076.
(36) Fan, S.; et al. A Na-rich fluorinated sulfate anti-perovskite with dual doping as solid electrolyte for Na metal solid state batteries. *Energy Storage Materials* **2020**, *31*, 87−94.
(37) Ippili, S.; et al. Halide double perovskite-based efficient mechanical energy harvester and storage devices for self-charging power unit. *Nano Energy* **2023**, *107*, No. 108148.
(38) Jaffari, G. H.; et al. Effect of temperature on structural phase transition and photoluminescence in organic-inorganic hybrid CH3NH3PbI3-xClx perovskite. *Opt. Mater.* **2023**, *142*, No. 114004.
(39) Yu, L.; et al. La0.4Sr0.6Co0.7Fe0.2Nb0.1O3-δ perovskite prepared by the sol-gel method with superior performance as a bifunctional oxygen electrocatalyst. *Int. J. Hydrogen Energy* **2020**, *45* (55), 30583−30591.
(40) Jiang, N.; et al. Super-hydrophilic electrode encapsulated lead halide-perovskite photoanode toward stable and efficient photo-electrochemical water splitting. *Chem. Eng. J.* **2024**, *492*, No. 152024.
(41) Dong, Z.; et al. Metal halide perovskites for CO2 photo-reduction: recent advances and future perspectives. *EES Catalysis* **2024**, *2* (2), 448−474.
(42) Li, Y.; et al. Photo-excited carrier behaviors of two-dimensional tin halide perovskite single crystals. *Cell Rep. Phys. Sci.* **2024**, *5*, No. 102020.
(43) Ünlü, F. Understanding the interplay of stability and efficiency in A-site engineered lead halide perovskites. *APL Materials* **2020**, DOI: 10.1063/5.0011851.
(44) Adeel, M.; et al. Synthesis and Characterization of Co−ZnO and Evaluation of Its Photocatalytic Activity for Photodegradation of Methyl Orange. *ACS Omega* **2021**, *6* (2), 1426−1435.
(45) Adams, D. J.; Churakov, S. V.; Cormack, A. N. Classification of perovskite structural types with dynamical octahedral tilting. *IUCrJ.* **2023**, *10*, 309−320.
(46) Klarbring, J. Low-energy paths for octahedral tilting in inorganic halide perovskites. *Phys. Rev. B* **2019**, *99* (10), No. 104105.
(47) Yang, T.; et al. Lead-free hybrid two-dimensional double perovskite with switchable dielectric phase transition. *Chin. Chem. Lett.* **2024**, *35*, No. 108707.
(48) Lian, L.; et al. Photophysics in Cs3Cu2 × 5 (X = Cl, Br, or I): Highly Luminescent Self-Trapped Excitons from Local Structure Symmetrization. *Chem. Mater.* **2020**, *32* (8), 3462−3468.
(49) Zhu, Y.; et al. In Situ Synthesis of Lead-Free Halide Perovskite−COF Nanocomposites as Photocatalysts for Photo-induced Polymerization in Both Organic and Aqueous Phases. *ACS Materials Lett.* **2022**, *4* (3), 464−471.
(50) Qi, K.; et al. Photocatalytic H2 generation via CoP quantum-dot-modified g-C3N4 synthesized by electroless plating. *Chinese Journal of Catalysis* **2020**, *41* (1), 114−121.
(51) Wang, J.; et al. Templated growth of oriented layered hybrid perovskites on 3D-like perovskites. *Nat. Commun.* **2020**, *11* (1), 582.
(52) Low, Y. J.; et al. Synthesis of cesium silver bismuth bromide double perovskite nanoparticles via a microwave-assisted solvothermal method. *Materials Today Chemistry* **2023**, *29*, No. 101477.
(53) Lu, H.; et al. Stable black-phase $FAPbI_3$ perovskite solar cells. *Science* **2020**, *370* (6512), No. eabb8985.
(54) Chen, Y.; et al. Strain engineering and epitaxial stabilization of halide perovskites. *Nature* **2020**, *577* (7789), 209−215.
(55) Karami, M.; et al. Enhanced antibacterial activity and photocatalytic degradation of organic dyes under visible light using cesium lead iodide perovskite nanostructures prepared by hydro-thermal method. *Sep. Purif. Technol.* **2020**, *253*, No. 117526.
(56) Huang, Q.; et al. Highly stable lead-free Cs2AgBiI6-GO composite photocatalysts for efficient organic pollutant degradation. *Journal of Environmental Chemical Engineering* **2023**, *11* (3), No. 109960.
(57) Laishram, D.; et al. Air- and water-stable halide perovskite nanocrystals protected with nearly-monolayer carbon nitride for CO2 photoreduction and water splitting. *Appl. Surf. Sci.* **2022**, *592*, No. 153276.
(58) Sadiq, S.; et al. Synthesis of Metal−Organic Framework-Based ZIF-8@ZIF-67 Nanocomposites for Antibiotic Decomposition and Antibacterial Activities. *ACS Omega* **2023**, *8* (51), 49244−49258.
(59) Kirakosyan, A.; et al. Self-aligned CH3NH3PbBr3 perovskite nanowires via dielectrophoresis for gas sensing applications. *Appl. Mater. Today* **2022**, *26*, No. 101307.
(60) Feng, D.; et al. Novel photoelectrochemical sensor for cholesterol based on CH3NH3PbBr3 perovskite /TiO2 inverse opal heterojunction coated with molecularly imprinted polymers. *Sens. Actuators, B* **2022**, *368*, No. 132121.
(61) Electronic supporting information (ESI) available: Materials and methods, NMR, crystal data, PFM, and solar cells. CCDC 2031849−2031850 and 2036182. For ESI and crystallographic data in

CIF or other electronic format see: Zhang, H.-Y.; Xiong, R.-G. Three-dimensional narrow-bandgap perovskite semiconductor ferroelectric methylphosphonium tin triiodide for potential photovoltaic application. *Chem. Commun.* **2023**, *59* (7), 920−923.
(62) Li, C.-T.; et al. All-inorganic lead-free halide perovskite Cs2TeBr6 enables real-time touchless human breath and finger related humidity monitoring. *Sens. Actuators, B* **2023**, *379*, No. 133240.
(63) Pantaler, M.; et al. Revealing Weak Dimensional Confinement Effects in Excitonic Silver/Bismuth Double Perovskites. *JACS Au* **2022**, *2* (1), 136−149.
(64) Chen, G.; et al. Lead-Free Halide Perovskite $Cs_3Bi_{2x}Sb_{2-2x}I_9$ (x ≈ 0.3) Possessing the Photocatalytic Activity for Hydrogen Evolution Comparable to that of $(CH_3NH_3)PbI_3$. *Advanced Materials* **2020**, *32* (39), No. 2001344.
(65) Wang, A.; et al. MOF-Derived Porous Carbon-Supported Bimetallic Fischer−Tropsch Synthesis Catalysts. *Ind. Eng. Chem. Res.* **2022**, *61* (11), 3941−3951.
(66) Pramod, A. K.; et al. Synthesis of lead-free Cs3Sb2Cl3Br6 halide perovskite through solution processing method for self-powered photodetector applications. *Mater. Lett.* **2022**, *306*, No. 130874.
(67) Wang, F.; et al. Iodine-assisted antisolvent engineering for stable perovskite solar cells with efficiency > 21.3%. *Nano Energy* **2020**, *67*, No. 104224.
(68) Vuong, V.-H.; et al. Flexible, stable, and self-powered photodetectors embedded with chemical vapor deposited lead-free bismuth mixed halide perovskite films. *Chem. Eng. J.* **2023**, *458*, No. 141473.
(69) Xia, P.; et al. Novel non-real-time stress recording strategy based on mechanochemically synthesized lead-free perovskite of Cs2TeCl6. *Chem. Eng. J.* **2023**, *470*, No. 144319.
(70) Ullah, S.; et al. Theoretical and experimental progress in photothermal catalysis for sustainable energy and environmental protection: Key problems and strategies towards commercialization. *Renewable and Sustainable Energy Reviews* **2024**, *201*, No. 114615.
(71) Mu, Y.-F.; et al. Lead-free halide perovskite hollow nanospheres to boost photocatalytic activity for CO2 reduction. *Appl. Catal. B: Environmental* **2023**, *338*, No. 123024.
(72) Nguyen, V. H.; et al. Dual-channel charge transfer over g−C3N4/g−C3N4/bismuth-based halide perovskite composite for improving photocatalytic degradation of tetracycline hydrochloride. *J. Alloys Compd.* **2023**, *965*, No. 171509.
(73) Li, K.; et al. Highly-efficient and stable photocatalytic activity of lead-free Cs2AgInCl6 double perovskite for organic pollutant degradation. *J. Colloid Interface Sci.* **2021**, *596*, 376−383.
(74) Azadinia, M.; et al. Maximizing the performance of single and multijunction MA and lead-free perovskite solar cell. *Materials Today Energy* **2021**, *20*, No. 100647.
(75) Eckhardt, K.; et al. A photosensor based on lead-free perovskite-like methyl-ammonium bismuth iodide. *Sensors and Actuators A: Physical* **2019**, *291*, 75−79.
(76) Mohanty, I. Synthesis and characterization of Methylammonium tin iodide (CH3NH3SnI3) absorber layer for photovoltaic applications. *Materials Today: Proceedings* **2023**, DOI: 10.1016/j.matpr.2023.05.677.
(77) Ur Rehman, J.; et al. First-principles calculations to investigate structural, electronics, optical and elastic properties of Sn-based inorganic Halide-perovskites CsSnX3 (X = I, Br, Cl) for solar cell applications. *Computational and Theoretical Chemistry* **2022**, *1209*, No. 113624.
(78) Mahmoudi, T.; et al. Suppression of Sn2+/Sn4+ oxidation in tin-based perovskite solar cells with graphene-tin quantum dots composites in active layer. *Nano Energy* **2021**, *90*, No. 106495.
(79) Wu, S.-C.; et al. Long-chain alkylammonium organic−inorganic hybrid perovskite for high performance rechargeable aluminon-ion battery. *Nano Energy* **2023**, *110*, No. 108273.
(80) Zhong, F.; et al. Ligand-mediated exciton dissociation and interparticle energy transfer on CsPbBr3 perovskite quantum dots for efficient CO2-to-CO photoreduction. *Science Bulletin* **2024**, *69* (7), 901−912.
(81) Zhang, Z.; et al. Mesoporous α-Fe2O3 nanostructures decorated with perovskite Cs3Bi2Br9 quantum dots as an S-scheme photocatalyst for efficient charge transfer and CO2 conversion. *Appl. Surf. Sci.* **2023**, *640*, No. 158468.
(82) Zhang, Y.; et al. Zero-Dimensional Cs4PbBr6 Perovskite Nanocrystals. *J. Phys. Chem. Lett.* **2017**, *8* (5), 961−965.
(83) Alqorashi, A. K.; et al. DFT insights into the stoichiometric (001), (011) and (111) thin film surfaces of Ba2NaIO6. *Solid State Commun.* **2024**, *387*, No. 115537.
(84) Qian, J.; et al. Mesoporous TiO2 matrix embeded with Cs2CuBr4 perovskite quantum dots as a step-scheme-based photocatalyst for boosting charge separation and CO2 photoconversion. *Appl. Surf. Sci.* **2024**, *648*, No. 159084.
(85) Mei, X.; et al. Stabilizing dynamic surface of highly luminescent perovskite quantum dots for light-emitting diodes. *Chem. Eng. J.* **2023**, *453*, No. 139909.
(86) Huo, B.; et al. Amino-mediated anchoring of FAPbBr3 perovskite quantum dots on silica spheres for efficient visible light photocatalytic NO removal. *Chem. Eng. J.* **2021**, *406*, No. 126740.
(87) Deng, J.; et al. Room-temperature synthesis of excellent-performance CsPb1-xSnxBr3 perovskite quantum dots and application in light emitting diodes. *Materials & Design* **2020**, *185*, No. 108246.
(88) Zhou, X.-M.; et al. Development of a rapid visual detection technology for BmNPV based on CRISPR/Cas13a system. *Journal of Invertebrate Pathology* **2024**, *203*, No. 108072.
(89) Liu, W.; et al. Luminescence, stability, and applications of CsPbBr3 quantum dot/poly(methyl methacrylate) composites prepared by a solvent- and ligand-free ball milling method. *Opt. Mater.* **2023**, *136*, No. 113398.
(90) Wang, Y.; et al. Electrochemically switchable electrochemiluminescent sensor constructed based on inorganic perovskite quantum dots synthesized with microwave irradiation. *J. Electroanal. Chem.* **2020**, *867*, No. 114181.
(91) Sial, M. A. Z. G.; et al. Electrochemical C-C coupling mediated by novel Sn-SnO2 supported Cu single atoms: The case of CO2 conversion to ethanol. *Chem. Eng. J.* **2024**, *489*, No. 151099.
(92) Yang, X.; et al. The efficient green light-emitting diodes based on low-toxicity Zr-Pb alloy perovskite quantum dots passivated by inorganic ligand. *Appl. Mater. Today* **2022**, *29*, No. 101658.
(93) Guo, T.; et al. Designed p-type graphene quantum dots to heal interface charge transfer in Sn-Pb perovskite solar cells. *Nano Energy* **2022**, *98*, No. 107298.
(94) Yang, H. S.; et al. Facile low-energy and high-yield synthesis of stable α-CsPbI3 perovskite quantum dots: Decomposition mechanisms and solar cell applications. *Chem. Eng. J.* **2023**, *454*, No. 140331.
(95) Lv, X. In-situ producing CsPbBr3 nanocrystals on (001)-faceted TiO2 nanosheets as S-scheme heterostructure for bifunctional photocatalysis. *J. Colloid Interface Sci.* **2023**, *652*, 673.
(96) Wang, X.; et al. Synthesis of ZnWO4/NiWO4 photocatalysts and their application in tetracycline hydrochloride degradation and antibacterial activities. *Journal of the Taiwan Institute of Chemical Engineers* **2024**, *157*, No. 105408.
(97) Cheng, R.; et al. Three-dimensional self-attaching perovskite quantum dots/polymer platform for efficient solar-driven CO2 reduction. *Materials Today Physics* **2021**, *17*, No. 100358.
(98) Electronic supporting information (ESI) available: Experimental details, temperature dependent tunability, photoluminescence quantum yield (PLQY) determination, EDX spectra, kinetic studies, recyclability test, TON calculation, CV spectra, quenching experiment, H2O2 detection, computational studies, HPLC spectra, 1H-NMR spectra, and 13C-NMR spectra. CIF. CCDC no. 2153616. For ESI and crystallographic data in CIF or other electronic format, see: Gurung, B.; et al. CsPbBr3 perovskite quantum dots as a visible light photocatalyst for cyclisation of diamines and amino alcohols: an efficient approach to synthesize imidazolidines, fused-imidazolidines

https://doi.org/10.1021/acsomega.4c04532
ACS Omega 2024, 9, 34220−34242

and oxazolidines. *Catalysis Science & Technology* **2022**, *12* (19), 5891−5898.
(99) Rasool, R. T.; et al. Nanoscaled MnSnO2@CsPbBr3 quantum dots heterostructure photocatalyst as efficient organic pollutants degradation by peroxymonosulfate; DFT calculation. *Journal of Materials Science & Technology* **2023**, *153*, 41−55.
(100) Khalid, H. D.; et al. Sustainable energy generation: High-performance NiCo2S4@S-g-C3N4 bifunctional electrocatalyst advances water splitting efficiency. *Int. J. Hydrogen Energy* **2024**, *68*, 128−138.
(101) Li, Y.; et al. Cs-Cu-Cl perovskite quantum dots for photocatalytic H2 evolution with super-high stability. *Appl. Catal. B: Environmental* **2023**, *337*, No. 122881.
(102) Getachew, G.; et al. Defect-passivated metal halide perovskite quantum dots stabilized into biodegradable porous polydopamine nanoparticles for photothermal/chemodynamic/gas therapy of cancer. *Chem. Eng. J.* **2023**, *467*, No. 143560.
(103) Hu, J.; et al. Solution-processed, flexible and broadband photodetector based on CsPbBr3/PbSe quantum dot heterostructures. *Journal of Materials Science & Technology* **2021**, *68*, 216−226.
(104) Muhammad, Z.; et al. Extrinsic n-type semiconductor transition in ZrSe2 with the metallic character through hafnium substitution. *J. Alloys Compd.* **2024**, *980*, No. 173616.
(105) Long, Z.; et al. All-inorganic halide perovskite (CsPbX3, X = Cl, Br, I) quantum dots synthesized via fast anion hot injection by using trimethylhalosilanes. *Ceram. Int.* **2022**, *48*, 35474−35479.
(106) Khan, A.; et al. Preparation of visible-light active MOFs-Perovskites (ZIF-67/LaFeO3) nanocatalysts for exceptional CO2 conversion, organic pollutants and antibiotics degradation. *Heliyon* **2024**, *10* (5), No. e27378.
(107) Zhao, L.; et al. Construction of Ultrathin S-Scheme Heterojunctions of Single Ni Atom Immobilized Ti-MOF and $BiVO_4$ for CO_2 Photoconversion of nearly 100% to CO by Pure Water. *Advanced Materials* **2022**, *34* (41), No. 2205303.
(108) Liu, C.; et al. In Situ Growth of Three-Dimensional MXene/Metal−Organic Framework Composites for High-Performance Supercapacitors. *Angew Chem Int Ed* **2022**, *61* (11), No. e202116282.
(109) Sadiq, S. A critical review on metal-organic frameworks (MOFs) based nanomaterials for biomedical applications: Designing, recent trends, challenges, and prospects. *Heliyon* **2024**, *10* (3), e25521.
(110) Helal, A.; et al. Defect-engineering a metal−organic framework for CO2 fixation in the synthesis of bioactive oxazolidinones. *Inorganic Chemistry Frontiers* **2020**, *7* (19), 3571−3577.
(111) Xu, Y.; et al. Controlling the electronic structure of Fe-MOF electrocatalyst for enhanced water splitting and urea oxidation: A plasma-assisted approach. *J. Colloid Interface Sci.* **2023**, *650*, 1290−1300.
(112) Hu, J.; et al. Fabrication of Ce-La-MOFs for defluoridation in aquatic systems: A kinetics, thermodynamics and mechanisms study. *Sep. Purif. Technol.* **2023**, *314*, No. 123562.
(113) Chen, C.; et al. Microwave-assisted synthesis of bimetallic NiCo-MOF-74 with enhanced open metal site for efficient CO2 capture. *Environmental Functional Materials* **2022**, *1* (3), 253−266.
(114) Asadi, A.; et al. Engineering water-stable metal halide perovskite/MOF-808 heterojunction through mechanochemical method: S-scheme photocatalytic system for multifunctional applications. *Materials Science in Semiconductor Processing* **2023**, *165*, No. 107707.
(115) Li, T.; et al. MOF-derived nano-popcorns synthesized by sonochemistry as efficient sensitizers for tumor microwave thermal therapy. *Biomaterials* **2020**, *234*, No. 119773.
(116) Zhao, L.; et al. The synthesis of interface-modulated ultrathin Ni(ii) MOF/g-C3N4 heterojunctions as efficient photocatalysts for CO2 reduction. *Nanoscale* **2020**, *12* (18), 10010−10018.
(117) Chen, H.; et al. Construction of ultra-high defective iron-based metal organic frameworks with small molecule acid regulator for enhanced degradation of sulfamethoxazole. *Journal of Cleaner Production* **2022**, *348*, No. 131367.
(118) Xi, Y.; et al. Aspect ratio dependent photocatalytic enhancement of CsPbBr3 in CO2 reduction with two-dimensional metal organic framework as a cocatalyst. *Appl. Catal. B: Environmental* **2021**, *297*, No. 120411.
(119) Ghanem, A. S.; et al. High gas permselectivity in ZIF-302/polyimide self-consistent mixed-matrix membrane. *J Applied Polymer Sci* **2020**, *137* (13), 48513.
(120) Ma, L.; et al. Self-assembled MOF microspheres with hierarchical porous structure for efficient uranium adsorption. *Sep. Purif. Technol.* **2023**, *314*, No. 123526.
(121) Xue, P.; et al. A MOF-Derivative Decorated Hierarchical Porous Host Enabling Ultrahigh Rates and Superior Long-Term Cycling of Dendrite-Free Zn Metal Anodes. *Advanced Materials* **2022**, *34* (14), No. 2110047.
(122) Hai, T.; et al. Designing g-C3N4/ZnCo2O4 nanocoposite as a promising photocatalyst for photodegradation of MB under visible-light excitation: Response surface methodology (RSM) optimization and modeling. *J. Phys. Chem. Solids* **2024**, *185*, No. 111747.
(123) Khan, M. Experimental and DFT study of GO-decorated CaO quantum dots for catalytic dye degradation and bactericidal potential. *Front. Environ. Sci.* **2023**, DOI: 10.3389/fenvs.2023.1158399.
(124) Liu, J.-L.; et al. sp2-c linked Cu-based metal-covalent organic framework for chemical and photocatalysis synergistic reduction of uranium. *Chem. Eng. J.* **2024**, *491*, No. 151982.
(125) Yang, J.; et al. 2D/3D covalent organic frameworks based on cobalt corroles for CO binding. *Materials Today Chemistry* **2023**, *28*, No. 101357.
(126) Khan, S.; et al. Eco-friendly graphitic carbon nitride nanomaterials for the development of innovative biomaterials: Preparation, properties, opportunities, current trends, and future outlook. *Journal of Saudi Chemical Society* **2023**, *27* (6), No. 101753.
(127) Dong, B.; et al. Ionic liquid as a green solvent for ionothermal synthesis of 2D keto-enamine-linked covalent organic frameworks. *Mater. Chem. Phys.* **2019**, *226*, 244−249.
(128) Maschita, J.; Banerjee, T.; Lotsch, B. V. Direct and Linker-Exchange Alcohol-Assisted Hydrothermal Synthesis of Imide-Linked Covalent Organic Frameworks. *Chem. Mater.* **2022**, *34* (5), 2249−2258.
(129) Ji, W.; et al. Rapid microwave synthesis of dioxin-linked covalent organic framework for efficient micro-extraction of perfluorinated alkyl substances from water. *J. Hazard. Mater.* **2020**, *397*, No. 122793.
(130) Guo, W.; et al. High efficient removal of U(VI) by covalent−organic frameworks fabricated by mechanochemical method: Adsorption process, mechanism and surface complexation modeling. *Journal of Environmental Chemical Engineering* **2023**, *11* (3), No. 109763.
(131) Khan, I.; et al. Non-covalent interaction of atomically dispersed dual-site catalysts featuring Co and Ni nascent pair sites for efficient electrocatalytic overall water splitting. *Journal of Materials Science & Technology* **2024**, *178*, 210−225.
(132) Khan, M. S.; et al. Electronic, magnetic and optical properties of Co(II) doped and (Al, Co) co-doped CdS nanowires: An ab initio study. *Materials Science in Semiconductor Processing* **2024**, *171*, No. 108019.
(133) Chen, Z.-k.; et al. Hsp90 could promote BmNPV proliferation by interacting with Actin-4 and enhance its expression. *Developmental & Comparative Immunology* **2023**, *142*, No. 104667.
(134) Fu, Y.; et al. Zwitterionic Covalent Organic Frameworks: Attractive Porous Host for Gas Separation and Anhydrous Proton Conduction. *ACS Nano* **2021**, *15* (12), 19743−19755.
(135) Su, Z.; et al. Multilayer structure covalent organic frameworks (COFs) linking by double functional groups for advanced K+ batteries. *J. Colloid Interface Sci.* **2023**, *639*, 7−13.
(136) Wu, Z.; et al. Metalation of functionalized benzoquinoline-linked COFs for electrocatalytic oxygen reduction and lithium-sulfur batteries. *J. Colloid Interface Sci.* **2023**, *650*, 1466−1475.

https://doi.org/10.1021/acsomega.4c04532
ACS Omega 2024, 9, 34220−34242

(137) Ren, J.; et al. Encapsulating all-inorganic perovskite quantum dots into mesoporous metal organic frameworks with significantly enhanced stability for optoelectronic applications. *Chem. Eng. J.* **2019**, *358*, 30−39.
(138) Shi, L.; et al. Facile in-situ preparation of MAPbBr3@UiO-66 composites for information encryption and decryption. *J. Solid State Chem.* **2020**, *282*, No. 121062.
(139) Mollick, S.; et al. A hybrid blue perovskite@metal−organic gel (MOG) nanocomposite: simultaneous improvement of luminescence and stability. *Chemical Science* **2019**, *10* (45), 10524−10530.
(140) Qiao, G.-Y.; et al. Perovskite Quantum Dots Encapsulated in a Mesoporous Metal−Organic Framework as Synergistic Photocathode Materials. *J. Am. Chem. Soc.* **2021**, *143* (35), 14253−14260.
(141) Li, Z. MOF-Confined Sub-2 nm Stable CsPbX(3) Perovskite Quantum Dots. *Nanomaterials (Basel)* **2019**, *9* (8), 1147.
(142) Wang, Y.-Y.; et al. Confining lead-free perovskite quantum dots in metal−organic frameworks for visible light-driven proton reduction. *Materials Chemistry Frontiers* **2021**, *5* (21), 7796−7807.
(143) Wang, Q.; et al. High-performance electrochemiluminescence sensors based on ultra-stable perovskite quantum dots@ZIF-8 composites for aflatoxin B1 monitoring in corn samples. *Food Chem.* **2023**, *410*, No. 135325.
(144) Zhao, Y.; et al. CsPbX3 Quantum Dots Embedded in Zeolitic Imidazolate Framework-8 Microparticles for Bright White Light-Emitting Devices. *ACS Appl. Nano Mater.* **2021**, *4* (5), 5478−5485.
(145) Ikram, M.; et al. Fabrication of La-Doped MoS2 Nanosheets with Tuned Bandgap for Dye Degradation and Antimicrobial Activities, Experimental and Computational Investigations. *Advanced Materials Interfaces* **2023**, *10* (14), No. 2202404.
(146) Wang, T.; et al. Room temperature nondestructive encapsulation via self-crosslinked fluorosilicone polymer enables damp heat-stable sustainable perovskite solar cells. *Nat. Commun.* **2023**, *14* (1), 1342.
(147) Ren, J.; Zhou, X.; Wang, Y. In situ passivation and thiol-mediated anchoring of perovskite quantum dots in mesoporous covalent-organic frameworks. *Chem. Eng. J.* **2023**, *454*, No. 140285.
(148) Yuan, G.; et al. Promoting charge separation in a composite of *δ*-CsPbI3 and covalent organic frameworks. *Journal of Materials Chemistry C* **2023**, *11* (23), 7570−7574.
(149) Xiao, K.; et al. Zinc−Air Battery-Assisted Self-Powered PEC Sensors for Sensitive Assay of PTP1B Activity Based on Perovskite Quantum Dots Encapsulated in Vinyl-Functionalized Covalent Organic Frameworks. *Anal. Chem.* **2022**, *94* (27), 9844−9850.
(150) Zhang, H.; et al. In situ growth strategy to construct perovskite quantum dot@covalent organic framework composites with enhanced water stability. *Nanotechnology* **2023**, *34* (24), No. 245601.
(151) Zhang, N.; et al. Visible-light driven boosting electron-hole separation in CsPbBr3 QDs@2D Cu-TCPP heterojunction and the efficient photoreduction of CO2. *J. Colloid Interface Sci.* **2022**, *608*, 3192−3203.
(152) Wu, L. Y.; et al. Encapsulating Perovskite Quantum Dots in Iron-Based Metal-Organic Frameworks (MOFs) for Efficient Photocatalytic CO(2) Reduction. *Angew. Chem., Int. Ed. Engl.* **2019**, *58* (28), 9491−9495.
(153) Rambabu, D.; et al. Stabilization of MAPbBr3 Perovskite Quantum Dots on Perovskite MOFs by a One-Step Mechanochemical Synthesis. *Inorg. Chem.* **2020**, *59* (2), 1436−1443.
(154) Kong, Z.-C.; et al. Core@Shell CsPbBr3@Zeolitic Imidazolate Framework Nanocomposite for Efficient Photocatalytic CO2 Reduction. *ACS Energy Lett.* **2018**, *3* (11), 2656−2662.
(155) Ding, L.; et al. Embedding Cs2AgBiBr6 QDs into Ce-UiO-66-H to in situ construct a novel bifunctional material for capturing and photocatalytic reduction of CO2. *Chem. Eng. J.* **2022**, *446*, No. 137102.
(156) Kour, P.; Mukherjee, S. P. CsPbBr3/Cs4PbBr6 perovskite@COF nanocomposites for visible-light-driven photocatalytic applications in water. *Journal of Materials Chemistry A* **2021**, *9* (11), 6819−6826.
(157) Zhang, D.; et al. Encapsulation of CH3NH3PbBr3 Perovskite Quantum Dots in MOF-5 Microcrystals as a Stable Platform for Temperature and Aqueous Heavy Metal Ion Detection. *Inorg. Chem.* **2018**, *57* (8), 4613−4619.
(158) Ahmed, S.; et al. Stable and highly luminescent CsPbX3 (X= Br, Br/Cl) perovskite quantum dot embedded into Zinc(II) imidazole-4,5-dicarboxylate metal organic framework as a luminescent probe for metal ion detection. *Mater. Chem. Phys.* **2023**, *295*, No. 127093.
(159) Yin, Z.; et al. Luminescent Dynamics of Perovskite Quantum Dots Encapsulated in Metal−Organic Frameworks. *J. Phys. Chem. C* **2023**, *127* (22), 10655−10661.
(160) Liu, Y.; et al. Synthesis of Imine-Based Covalent Organic Frameworks Catalyzed by Metal Halides and in Situ Growth of Perovskite@COF Composites. *ACS Materials Lett.* **2020**, *2* (12), 1561−1566.
(161) Bhattacharyya, S.; Rambabu, D.; Maji, T. K. Mechanochemical synthesis of a processable halide perovskite quantum dot−MOF composite by post-synthetic metalation. *Journal of Materials Chemistry A* **2019**, *7* (37), 21106−21111.
(162) Feng, S.; et al. Modifying CsPbX3 (X = Cl, Br, I) with a Zeolitic Imidazolate Framework through Mechanical Milling for Aqueous Photocatalytic H2 Evolution. *ACS Appl. Energy Mater.* **2022**, *5* (5), 6248−6255.
(163) Zhang, X.; et al. Additional electron transfer channels of thermostable 0D Cs(Pb: Pt)Br3 perovskite quantum dots /2D accordion-like Ni-MOF nanojunction for photocatalytic H2 evolution. *Int. J. Hydrogen Energy* **2022**, *47* (97), 40860−40871.
(164) Xie, Z.; et al. In situ confined growth of ultrasmall perovskite quantum dots in metal−organic frameworks and their quantum confinement effect. *Nanoscale* **2020**, *12* (32), 17113−17120.
(165) Nguyen, T. M. H.; Bark, C. W. Synthesis of Cobalt-Doped TiO2 Based on Metal−Organic Frameworks as an Effective Electron Transport Material in Perovskite Solar Cells. *ACS Omega* **2020**, *5* (5), 2280−2286.
(166) Qiao, G. Y.; et al. Perovskite Quantum Dots Encapsulated in a Mesoporous Metal-Organic Framework as Synergistic Photocathode Materials. *J. Am. Chem. Soc.* **2021**, *143* (35), 14253−14260.
(167) Ren, J.; Zhou, X.; Wang, Y. Dual-emitting CsPbX3@ZJU-28 (X = Cl, Br, I) composites with enhanced stability and unique optical properties for multifunctional applications. *Chem. Eng. J.* **2020**, *391*, No. 123622.
(168) Singh, A. K.; et al. Probing reversible photoluminescence alteration in CH3NH3PbBr3 colloidal quantum dots for luminescence-based gas sensing application. *J. Colloid Interface Sci.* **2019**, *554*, 668−673.
(169) Jiang, X.; et al. Multiple Interpenetrating Metal−Organic Frameworks with Channel-Size-Dependent Behavior for Selective Gossypol Detection and Perovskite Quantum Dot Encapsulation. *ACS Appl. Mater. Interfaces* **2022**, *14* (44), 49945−49956.
(170) Zhu, S.; et al. Novel cubic gravel-like EDAPbCl4@ZIF-67 as electrochemical sensor for the detection of protocatechuic acid. *J. Alloys Compd.* **2022**, *903*, No. 163946.
(171) Ye, W.; et al. Halide Perovskite glues activate two-dimensional covalent organic framework crystallites for selective NO2 sensing. *Nat. Commun.* **2023**, *14* (1), 2133.
(172) Ahmed, S.; et al. A hierarchically porous MOF confined CsPbBr3 quantum dots: Fluorescence switching probe for detecting Cu (II) and melamine in food samples. *J. Photochem. Photobiol., A* **2023**, *443*, No. 114821.
(173) Ahmad, I.; et al. Surface crafting and entrapment of CsPbBr3 perovskite QDs in ZIF-8 for ammonia recognition. *Spectrochimica Acta Part A: Molecular and Biomolecular Spectroscopy* **2023**, *302*, No. 123091.
(174) He, J.; et al. In Situ Synthesized 2D Covalent Organic Framework Nanosheets Induce Growth of High-Quality Perovskite Film for Efficient and Stable Solar Cells. *Adv Funct Materials* **2022**, *32* (16), No. 2110030.

https://doi.org/10.1021/acsomega.4c04532
ACS Omega 2024, 9, 34220−34242

(175) Mohamed, M. G.; et al. Exploitation of two-dimensional conjugated covalent organic frameworks based on tetraphenylethylene with bicarbazole and pyrene units and applications in perovskite solar cells. *Journal of Materials Chemistry A* **2020**, *8* (22), 11448−11459.
(176) Zhang, Y.-N.; et al. MOF-derived ZnO as electron transport layer for improving light harvesting and electron extraction efficiency in perovskite solar cells. *Electrochim. Acta* **2020**, *330*, No. 135280.
(177) Zhang, Y.; et al. Spontaneous Formation of Lead-Free $Cs_3Cu_2I_5$ Quantum Dots in Metal−Organic-Frameworks with Deep-Blue Emission. *Small* **2022**, *18* (22), No. 2107161.
(178) Khan, I.; et al. Efficient Visible-Light Activities of TiO2 decorated and Cr3+incorporated-porous SmFeO3 for CO2 conversion and 4-chlorophenol degradation. *Surfaces and Interfaces* **2022**, *34*, No. 102358.
(179) Khan, I.; et al. Graphitic Carbon Nitride Composites with Gold and ZIF-67 Nanoparticles as Visible-Light-Promoted Catalysts for CO2 Conversion and Bisphenol A Degradation. *ACS Appl. Nano Mater.* **2022**, *5* (9), 13404−13416.
(180) Meng, L.; Qu, Y.; Jing, L. Recent advances in BiOBr-based photocatalysts for environmental remediation. *Chin. Chem. Lett.* **2021**, *32* (11), 3265−3276.
(181) Khan, I.; et al. Green synthesis of SrO bridged LaFeO3/g-C3N4 nanocomposites for CO2 conversion and bisphenol A degradation with new insights into mechanism. *Environmental Research* **2022**, *207*, No. 112650.
(182) Khan, I.; et al. Enhanced visible-light photoactivities of porous LaFeO3 by synchronously doping Ni2+ and coupling TS-1 for CO2 reduction and 2,4,6-trinitrophenol degradation. *Catalysis Science & Technology* **2021**, *11* (20), 6793−6803.
(183) Chen, S.; et al. Improved photoactivities for CO2 conversion and phenol degradation of α-Fe2O3 nanoparticles by co-coupling nano-sized BiPO4 and CuO to modulate electrons. *J. Alloys Compd.* **2019**, *800*, 231−239.
(184) Yaseen, M.; et al. Simultaneous operation of dibenzothiophene hydrodesulfurization and methanol reforming reactions over Pd promoted alumina based catalysts. *Journal of Fuel Chemistry and Technology* **2012**, *40* (6), 714−720.
(185) Hayat, A.; et al. Conjugated Electron Donor−Acceptor Hybrid Polymeric Carbon Nitride as a Photocatalyst for CO2 Reduction. *Molecules* **2019**, *24* (9), 1779.
(186) Khan, I.; et al. Bio-capped and green synthesis of ZnO/g-C3N4 nanocomposites and its improved antibiotic and photocatalytic activities: An exceptional approach towards environmental remediation. *Chinese Journal of Chemical Engineering* **2023**, *56*, 215−224.
(187) Saeed, M.; et al. Synthesis of p-n NiO-ZnO heterojunction for photodegradation of crystal violet dye. *Alexandria Engineering Journal* **2023**, *65*, 561−574.
(188) Zhang, C.; et al. Based on Z-scheme heterojunction $CsPbBr_3$/UiO-66 composite photocatalytic degradation. *Applied Organom Chem.* **2023**, *37* (7), No. e7122.
(189) Khan, S.; et al. Eriobotrya japonica assisted green synthesis of g-C3N4 nanocomposites and its exceptional photoactivities for doxycycline and rhodamine B degradation with mechanism insight. *J Chinese Chemical Soc* **2021**, *68* (11), 2093−2102.
(190) Saad, M.; et al. Development of stable S-scheme 2D−2D g-C3N4/CdS nanoheterojunction arrays for enhanced visible light photomineralisation of nitrophenol priority water pollutants. *Sci. Rep.* **2024**, *14* (1), 2897.
(191) Saeed, M.; et al. Synthesis of a visible-light-driven Ag2O−Co3O4 Z-scheme photocatalyst for enhanced photodegradation of a reactive yellow dye. *New J. Chem.* **2022**, *46* (48), 23297−23304.
(192) Khan, I.; et al. Synthesis of phosphate-bridged g-C3N4/LaFeO3 nanosheets Z-scheme nanocomposites as efficient visible photocatalysts for CO2 reduction and malachite green degradation. *Appl. Catal. A: General* **2022**, *629*, No. 118418.
(193) Mollick, S.; et al. Ultrastable Luminescent Hybrid Bromide Perovskite@MOF Nanocomposites for the Degradation of Organic Pollutants in Water. *ACS Appl. Nano Mater.* **2019**, *2* (3), 1333−1340.
(194) Saeed, M. Synthesis of p-n CoO-ZnO Heterojunction for Enhanced Visible-Light Assisted Photodegradation of Methylene Blue. *New J. Chem.* **2022**, *46*, 2224.
(195) Ali, S.; et al. Synthesis of activated carbon-supported TiO2-based nano-photocatalysts with well recycling for efficiently degrading high-concentration pollutants. *Catal. Today* **2019**, *335*, 557−564.
(196) Saeed, M. Enhanced photo catalytic degradation of methyl orange using p−n Co3O4-TiO2 hetero-junction as catalyst. *International Journal of Chemical Reactor Engineering* **2020**, DOI: 10.1515/ijcre-2020-0004.
(197) Zhang, S. Construction of 1D Ag-AgBr/AlOOH Plasmonic Photocatalyst for Degradation of Tetracycline Hydrochloride. *Front. Chem.* **2020**, DOI: 10.3389/fchem.2020.00117.
(198) Sun, N.; et al. Efficiently photocatalytic degradation of monochlorophenol on in-situ fabricated BiPO4/β-Bi2O3 heterojunction microspheres and O2-free hole-induced selective dechloridation conversion with H2 evolution. *Appl. Catal. B: Environmental* **2020**, *263*, No. 118313.
(199) Usman, M.; et al. Highly selective and stable hydrogenation of heavy aromatic-naphthalene over transition metal phosphides. *Science China Chemistry* **2015**, *58* (4), 738−746.
(200) Bahadur, A. Magnetic, Electronic, and Optical Studies of Gd-Doped WO(3): A First Principle Study. *Molecules* **2022**, *27* (20), 6976.
(201) Zhao, K.; et al. Ionic liquid assisted preparation of phosphorus-doped g-C3N4 photocatalyst for decomposition of emerging water pollutants. *Mater. Chem. Phys.* **2020**, *253*, No. 123322.
(202) Nie, W.; Tsai, H. Perovskite nanocrystals stabilized in metal−organic frameworks for light emission devices. *Journal of Materials Chemistry A* **2022**, *10* (37), 19518−19533.
(203) Jeong, J.; et al. Pseudo-halide anion engineering for α-FAPbI3 perovskite solar cells. *Nature* **2021**, *592* (7854), 381−385.
(204) Ma, D.; et al. Suppressed Phase Separation of Mixed-Halide Perovskite Quantum Dots Confined in Mesoporous Metal Organic Frameworks. *Nanomaterials* **2023**, *13* (10), 1655.

https://doi.org/10.1021/acsomega.4c04532
ACS Omega 2024, 9, 34220−34242